

REVIEW

CrossMark
click for updatesCite this: *RSC Adv.*, 2016, 6, 77410

Photochemical radical thiol–ene click-based methodologies for silica and transition metal oxides materials chemical modification: a mini-review

Andrea V. Bordoni, M. Verónica Lombardo and Alejandro Wolosiuk*

Although known for more than 40 years in the polymer chemistry field, the photochemical radical thiol–ene addition (PRTEA) has been recently recognized as a chemical reaction with click characteristics. Photoinitiation enables spatial and temporal control of this highly efficient reaction, bridging simple organic chemistry with high-end materials synthesis and surfaces functionalization. In this minireview, we focus on the latest contributions based on the PRTEA for the synthesis of chemical precursors for silica and transition metal oxides (TMO) based materials. We summarize the mechanism of the PRTEA, the development of new families of photoinitiators and how this extremely simple approach has spilled over into the materials science arena with clear success. In particular, PRTEA adds to the collective efforts for building a reliable and straightforward chemical toolbox for surface modification and the production of sol–gel precursors, nanoparticles and thin films. The excellent perspectives for simple molecular and supramolecular building block synthesis opens up a rational synthetic route for the design and integration of these components in multipurpose platforms.

Received 21st April 2016

Accepted 30th July 2016

DOI: 10.1039/c6ra10388j

www.rsc.org/advances

1. Introduction

The proper chemical functionalization of materials and surfaces is essential for countless technological applications where interfaces play a key role.¹ Diverse processes and products like corrosion protection, medical implants, heterogeneous chemical catalysis or adsorption of hazardous wastes require the surface anchoring of specific functional chemical groups that impart special properties to interfaces, from superhydrophobicity to molecular biorecognition and sensing.^{2–7} Moreover, tailored surface functional chemical groups are indispensable for the connectivity of different molecular-building blocks, as they orient the synthesis and design of advanced materials.⁸ In this context, the scientific design of novel materials relies on a “molecular and supramolecular spice rack” of diverse building blocks: from biological to inorganic components, from enzymes to semiconductors and metals.⁸ Thus, there is a growing necessity for simple chemical reactions for assembling and linking diverse components in a rational and hierarchical manner. Characteristics such as functionality, modularity, and connectivity will also modulate the physicochemical properties of the material, be it a thin film, a nanoparticle dispersion, or a composite powder.⁹ As part of this multidisciplinary effort, the control of molecular interactions for the construction of specific molecular architectures is

a common objective shared by organic and inorganic chemists, materials scientists, biochemists and polymer chemists. In summary, the options for grafting or chemically modifying the surface or the constituent molecular building blocks remains a challenging arena with technological consequences.¹⁰

Organoalkoxysilanes are molecules with the general formula $R'_n\text{Si}(\text{OR})_{4-n}$ that have revolutionized the manufacture of everyday materials and are key intermediates in sol–gel processing, as molecular precursors for building blocks or for the chemical functionalization of oxide materials.^{11,12} The hydrolysis of the R group (*i.e.* methoxy, ethoxy) leads to a Si–O–Si polycondensed network that can form strong covalent bonds to hydroxylated surfaces, such as SiO₂ and transition metal oxides (TMO), making them particularly useful for connecting and bridging inorganic and organic components. The non-hydrolyzable organofunctional group R' (*i.e.* amino, cyano, methyl or vinyl groups) integrates to the Si–O–Si framework, either on its surface or within the SiO₂ or TMO based structure. In the case of surface functionalization, this advantageous characteristic allows keeping the texture of the supporting material (particles, powders, plain surfaces) while their bulk properties (density, refractive index, magnetism) remain intact. Alternatively, these chemical moieties can blend on the molecular scale, resulting in hybrid materials and nanocomposites with tailored properties and applications. In fact, SiO₂ based materials hold interesting promise for smart coatings, encapsulation, biomedical applications, photonics and as platforms for the synthesis of fine chemicals. In order to satisfy these requirements, the production of a versatile organo-

Gerencia Química – Centro Atómico Constituyentes, Comisión Nacional de Energía Atómica, CONICET, Av. Gral. Paz 1499, B1650KNA San Martín, Buenos Aires, Argentina. E-mail: wolosiuk@cnea.gov.ar

alkoxysilanes library of chemical precursors needs a simple and effective coupling chemistry.^{13–18}

2. Click and click-derived chemistry

Click chemistry has emerged in the last few years as a “pocket knife multi-tool”, based on a set of highly reliable and effective chemical reactions. This concept introduced by Sharpless *et al.* in 2001 states that “...The [click] reaction must be modular, wide in scope, give very high yields, generate only inoffensive by products that can be removed by nonchromatographic methods, and be stereospecific (but not necessarily enantioselective). The required process characteristics include simple reaction conditions (ideally, the process should be insensitive to



Andrea V. Bordoni obtained her degree in chemistry at the Facultad de Ciencias Exactas y Naturales of the Universidad de Buenos Aires (2004, FCEN-UBA). In 2010, she obtained her PhD in DQO, (FCEN-UBA), in the area of carbohydrates synthesis. Between 2011 and 2013, she carried out a postdoc under the direction of Dr Alejandro Wolosiuk (CNEA) and Dr Alberto Regazzoni (CNEA), focusing on the synthesis of mesoporous nanoparticles and surface chemical modification. Since 2013, she is a CONICET fellow.

M. Verónica Lombardo obtained her degree in Chemistry in 2007 (FCEN-UBA) and her PhD in Science and Technology, Chemistry Mention in 2014 (UNSAM). During her PhD thesis, she developed hybrid mesoporous materials for secondary recovery of divalent ions. Her scientific interest focuses on the confinement effect on the surface properties of functionalized mesoporous oxides.

Alejandro Wolosiuk studied chemistry at FCEN-UBA (Argentina), receiving his PhD in 2002. He carried on a postdoctoral stay at the University of Illinois at Urbana-Champaign (Department of Materials Science and Engineering). Since 2006, he is a research fellow of CONICET and Comisión Nacional de Energía Atómica (CNEA). His research interests include synthesis of colloids and nanoparticle materials, nanostructured hybrid interfaces, and the combination of chemically simple building blocks for applications in adsorption and sensing. More information can be found at: <http://qnano.com.ar/>.

oxygen and water), readily available starting materials and reagents, the use of no solvent or a solvent that is benign (such as water) or easily removed, and simple product isolation. Purification – if required – must be by nonchromatographic methods, such as crystallization or distillation, and the product must be stable under physiological conditions...”.¹⁹ Since then, several chemical reactions that fulfil the click philosophy have appeared or have been revisited: Diels–Alder cycloaddition, copper catalysed azide–alkyne cycloaddition (CuAAC) and modifications, nucleophilic ring-opening reactions of strained heterocycles (epoxides, aziridine, *etc.*), radical and nucleophilic thiol–ene addition reactions, oxime ligations and nitroxide radical coupling, just to name a few.²⁰ As pointed out by Lahann, initially, the click chemistry concept was thought to be fundamental in the drug discovery field; however, this notion very soon spilled over into materials science, polymer chemistry and biotechnology with clear success.²¹ This unexpected outcome has forced the revision of the click terminology. In fact, Espeel and Du Prez highlighted the recent development of “click-inspired”, “click-based” or “click-derived” synthetic methodologies.²⁰ This necessary rephrasing specifically points to potential approaches for chemical modifications that share some of the principles stated by Sharpless: orthogonality, modularity, straightforward chemistry ligation procedures or energetically “spring-loaded” chemical reactions.¹⁹ Given that diverse chemistry fields have embraced this methodology, each of them set specific constraints and look for certain advantages when considering a click reaction. For instance, there are clear differences between the processes and workup involved in surface materials modification and polymer synthesis. The former, which in some cases (*i.e.* surface or inorganic monolith modification), does not require any purification steps and reaction yields, with a few exceptions, is hardly considered; the straightforward anchoring of molecules with fast kinetics and orthogonality are mainly considered. On the other hand, polymer synthesis is forced to deal with purification and separation of polymer mixtures as a necessary step in order to get pure products.²² Obviously, this situation calls for click reactions that must satisfy all conditions stated by Sharpless.

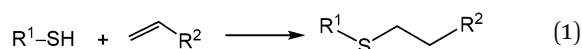
Among the “click-toolbox”, the photochemical radical thiol–ene addition (PRTEA) has attracted much interest, as it is easy to perform, is versatile in the availability of reactants and the mild reaction conditions required make it compatible with most functional groups.²³ This reaction, known from the late 70s, has the following characteristics: (a) is orthogonal to most organic functional groups (–COOH, –NH₂, –CH₂OH), (b) does not require O₂ free or anhydrous conditions, (c) benefits from the vast commercial availability of both thiol compounds, aimed at Au surfaces functionalization, and –ene based molecules, for olefin polymer synthesis, (d) the photochemical initiation of the reaction is highly attractive for tailored patterned surface modification and (e) solvents can be minimized, where reactions are carried under neat conditions.^{24,25}

In this context, we will address click-derived approaches, based on the PRTEA reaction, for the simple chemical modification of a variety of inorganic oxide materials (*i.e.* SiO₂ and Fe₃O₄) and surfaces, that may not satisfy all click requirements,

but, open a new venue for tailoring surfaces and materials in a direct and simple manner.

2.1 General aspects of radical thiol-ene click reactions

The thiol-ene radical reaction involves the addition of a thiol across an alkene molecule, also known as hydrothiolation, as schematized in the following reaction:



A more detailed mechanistic analysis is depicted in Scheme 1: (i) the reaction is initiated thermally or photochemically after H abstraction from a thiol molecule using a radical initiator; this generates a highly reactive thiyl radical ($\text{R}_1\text{S}^\bullet$) that efficiently attacks alkene molecules ($\text{R}_2\text{CH}_2=\text{CH}$); (ii) the generated carbon-centered radical ($\text{R}_1\text{SCH}_2\text{C}^\bullet\text{HR}_2$) is also able to abstract a H from a R_1SH molecule. This last step can be considered as an amplification stage, where a single thiyl radical causes a cascade of chemical attacks, similar to chain-growth free radical polymerizations. From a historical perspective, this characteristic, in addition to a fast kinetic reaction, has been fuelling the research on thiol-ene polymerizations for more than 70 years.²⁶

The rate of the radical thiol-ene addition is highly dependent on molecular characteristics such as electron density of the alkene, the S-H bond strength and the hydrogen abstraction ability of the intermediate carbon-centered radical. To date, alkene structure has been extensively studied related to the kinetic parameters of the reaction;²⁷ as a rule of thumb, the following reactivity order applies: norbornene > vinyl ether > propenyl > alkene > vinyl ester > *n*-vinyl amides > allyl ether > allyl triazine > *n*-vinyl amides > allylether > allyl triazine > allyl isocyanurate > acrylate > unsaturated ester > *n*-substituted malimide > acrylonitrile > methacrylate > styrene > conjugated dienes.²⁶ On the other side, when analyzing thiol reactivity, the electrophilicity of the thiyl radicals is essential.²³ Nonetheless, alkyl-3-thiolpropionates and alkylthioglycolates (*i.e.* thiol glycolate) stand out as multifunctional reactants for thiol-ene

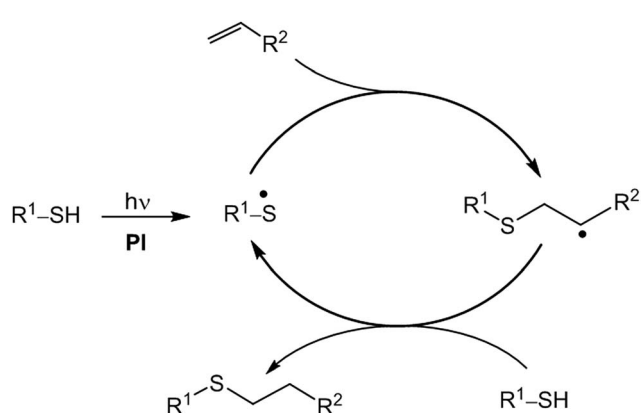
polymerizations. Apparently, these molecules react faster than alkylthiols because of the weakening of the S-H bond, due to hydrogen bonding with the carbonyl group.²⁶

Despite the apparent simplicity of this reaction, it is very important to differentiate the potential pathway reactions that the thiol-ene addition can take. An overlooked fact, that may bring confusion to beginners, is to distinguish between thiol-ene Michael addition and radical thiol-ene reactions. Both transformations involve hydrothiolation of the -ene bond, differing in the mechanism and the chemical nature of the intermediate species. The Michael addition involves the heterolytic cleavage of the -SH bond, forming a negatively charged nucleophile ($-\text{S}^-$). In this context, as thiols are acid-base groups too, they can produce thiolate species that can act as soft nucleophiles. Considering the rich chemistry of the SH group, it is fundamental to control the reaction conditions according to the thiol structure, as this will favour one mechanism over the other.^{23,28} Obviously, the thiol-ene Michael addition expands the library of thiol/alkene compounds and complements the possible shortcomings of the radical thiol-ene reaction. For nucleophilic/base thiol-ene addition, we suggest that the reader check other reviews that illustrate the use and applications of the thiol-ene Michael addition.²⁹

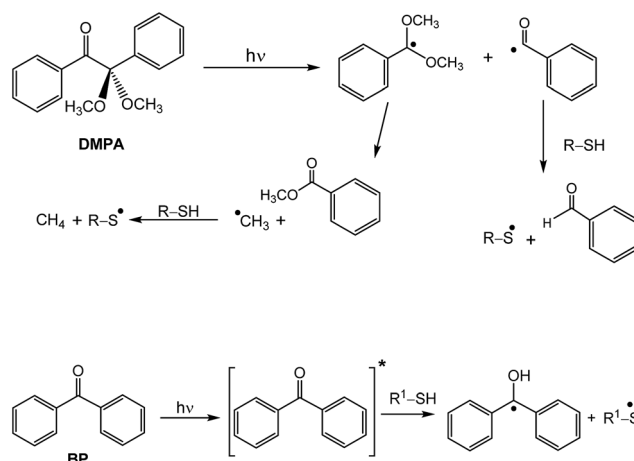
As a final note, we must emphasize that contrary to what is observed in most radical-induced crosslinking processes, the thiol-ene radical reaction is not inhibited by oxygen. The peroxy radicals (PO_2^\bullet) formed by O_2 scavenging, can also react with the thiol and contribute to the propagation of the chain reaction.³⁰ This has been stressed as one of the major advantages of the radical thiol-ene click reaction and definitively impacts at the industrial scale for mass production, simplifying the experimental lab setup.

2.2 Photochemical radical thiol-ene click reactions

Photochemical reactions open the possibility to use conventional photolithography masks in order to transfer an arbitrary pattern and therefore, localize different surface chemistries in



Scheme 1 The photochemical radical-mediated thiol-ene reaction mechanism.



Scheme 2 Mechanism for the photoinitiation of a cleavage-type photoinitiator (DMPA) and H-transfer photoinitiator (BP). Adapted from ref. 26.

2-D or 3-D fashion. The light intensity and exposure time can be easily controlled, enabling the use of UV-visible photons as a spatial and temporal synthesis director for surface modification. A natural consequence is that the results of the combination of thin film synthetic procedures with lithographic techniques are attractive for chemically patterned sensors mass production, MEMS devices, lab-on-chip setups and separation devices.^{31,32}

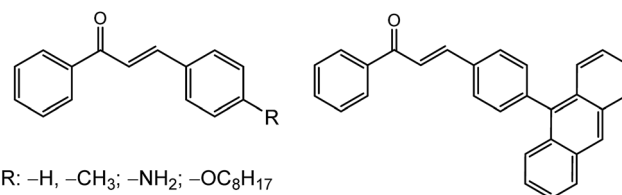
The mechanism for the photochemically initiated thiol-ene reactions is the same as for their thermal radical counterpart, involving the addition of a thiol across an alkene to give a thioether.²³ However, the distinctive feature of this approach is the use of light for thiol production, which can be highly localized in time and space. There are several methods for RS[•] production, which we will review below.

2.2.1 Photoinitiators

2.2.1.1 Direct photoinitiation. The simplest way to initiate the PRTEA is to generate thiyl free radicals (RS[•]) in a homolytic cleavage process.³³ Typically, most RS[•] radicals can be generated using wavelengths between 200 and 250 nm; although irradiation above 300 nm is inefficient, under continuous illumination, it can slowly generate a steady-state concentration of radicals that lowers termination reactions. Despite the apparent simplicity of this method, increased exposure times and high energy photons are required, compromising the stability of the molecules involved.

2.2.1.2 Molecular photoinitiators. A more efficient route for RS[•] production relies on the light excitation of photoinitiators (PI). In general, PI can be classified in two groups: (i) cleavage photoinitiators, such as 2,2-dimethoxy-1,2-diphenylethan-1-one (DMPA) and (ii) H-transfer photoinitiators, like benzophenone (BP).²⁶ In the former, DMPA gives a benzoyl radical and a tertiary carbon radical, as depicted in Scheme 2, which can insert directly into a carbon-carbon alkene bond or abstract a hydrogen atom from a thiol group. This starts the two-step process, characteristic of the thiol-ene free-radical chain reaction. On the other hand, hydrogen-transfer (abstraction) photoinitiators, such as BP, are less efficient due to a lower quantum yield for the production of reactive radicals.³⁴ Despite this apparent deficiency, BP is highly utilized in the varnish and inks industries, as it is very cost effective, having a low melting point that enables liquid pair eutectic formation with other PI.^{35,36} DMPA and BP are the most widely used PI for PRTEA.

Although UV photoinitiation is the standard procedure for thiol production, shifting the excitation wavelength to lower energies brings the possibility to use safer excitation sources. Several groups have directed their efforts to synthesizing novel molecules, with red-shifted excitation wavelengths, motivated by the widespread availability of light emitting diodes (LED) technologies.³⁷⁻⁴¹ Recently, Tehfe *et al.* generated thiyl radicals using chalcone derivatives (Scheme 3), evidenced by ESR spin trapping, and produced by means of a LED diode laser at 457 nm, a blue LED bulb at 462 nm, and a halogen lamp or sunlight.⁴² Shifting to longer wavelengths is promising for the immobilization of biologically derived molecules. Although this subject is in the early stages of development, it is expected to



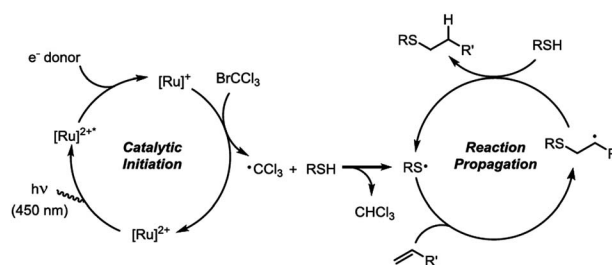
Scheme 3 Chalcone derivatives photoinitiators.⁴²

have a beneficial impact on PRTEA processes that require “soft” radical initiation.⁴³

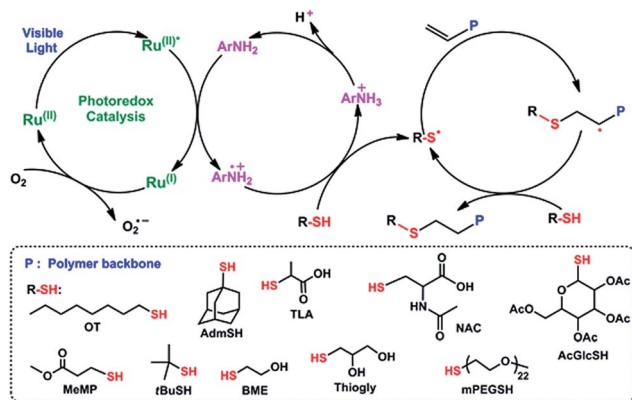
Visible light photoredox catalysis is another recent strategy that enables “green” organic transformations at ambient temperatures and using low energy photons.^{44,45} Ruthenium complex redox initiators, such as Ru(bpy)₃²⁺, are commonly employed because they show amphoteric redox activity in the form of reductive or oxidative cycles.^{44,46,47} As shown in Scheme 4, the excitation of Ru(bpy)₃²⁺ ions with visible light generates a [Ru(bpy)₃²⁺]* photoexcited state, through metal-to-ligand charge transfer (MLCT), that is further converted to [Ru(bpy)₃]⁺ with the aid of a reductant (*i.e.* an electron donor like sodium ascorbate). The generated [Ru(bpy)₃]⁺ can be oxidized again to Ru(bpy)₃²⁺ through an electron acceptor such as bromotrichloromethane.⁴⁶ Then, the produced trichloromethyl radical initiates the thioether bond formation by hydrogen atom abstraction from the thiol molecule. Subsequent capture of the electrophilic thiyl radical by an alkene produces a carbon-centered radical that, upon H-atom abstraction from another thiol molecule, propagates the radical chain process.

Xu *et al.* used a blue LED ($\lambda_{\text{max}} = 461$ nm), a Ru based complex, and *p*-toluidine for thiyl production as presented in Scheme 5.⁴⁷ Linear polymers were synthesized in a few minutes by step-growth addition reactions using 25 ppm photocatalyst relative to alkene concentration. The authors claim that this will have important industrial implications, as mild reaction conditions are required and it can be easily scaled-up.

Recently, Ma *et al.* reported the use of a *fac*-Ir(ppy)₃ photoredox catalyst for the α,ω -divinyl linear telechelic polythioether oligomers between 1,4-benzenedimethanethiol (BDMT) to diethylene glycol divinyl ether (DEGVE) after excitation at 380 nm.⁴⁸



Scheme 4 Proposed photocatalytic mechanism for [Ru(bpy)₃]²⁺ and BrCCl₃ mediated thiol-ene reaction. Reproduced with permission from Keylor *et al.*, *Tetrahedron* 2014, 70, 4264–4269. Copyright 2014 Elsevier B.V.



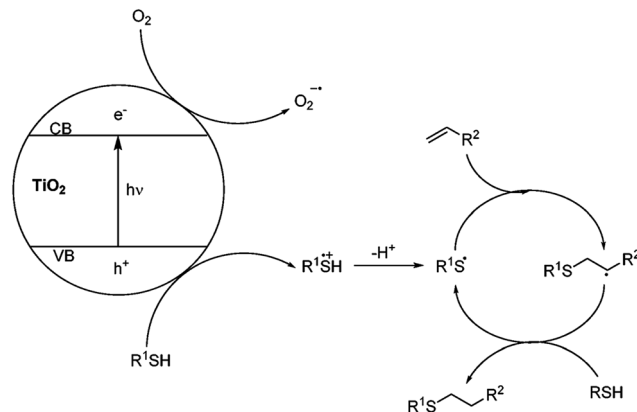
Scheme 5 Proposed photocatalysis mechanism for $[\text{Ru}(\text{bpy})_3]^{2+}$ and *p*-toluidine mediated thiol-ene reaction. Reproduced under Creative Commons Attribution 4.0 International Public License from Xu *et al.*, *Macromolecules*, 2015, **48**, 520–529.

2.2.1.3 Nanoparticle-based photoinitiators. Within the context of “green chemistry”, heterogeneous catalysts for chemical synthesis and transformations represent an exquisite choice in terms of reusability, sustainability, and easy separation from reaction containers; evidently, these characteristics fit very well with the click chemistry concept. Moreover, nanoparticle-based heterogeneous photoredox catalysts for free radical generation hold an interesting promise, since they can be easily recovered and have increased surface/mass ratios improving reaction yields or kinetics. Different materials are currently under investigation: from semiconductors (CdS, ZnS) and transition metal oxide (TiO_2 , Bi_2O_3 , Fe_2O_3 , Nb_2O_5 and ZnO), to plasmonic metal nanoparticles (Au, Ag) and polymeric graphitic carbon nitride ($\text{g-C}_3\text{N}_4$).^{49,50}

A very interesting recent application of heterogeneous photoredox catalysts is the use of nanoparticles for thiyl generation. Greaney's group used Aeroxide® P25 TiO_2 nanoparticles for producing photoexcited electron/hole pairs that lead to thiyl radicals.⁵¹ They suggest that O_2 must be present in solution to act as a sacrificial electron acceptor, after photo-excitation of electrons to the conduction band of the TiO_2 catalyst. Simultaneously, the hole in the valence band of TiO_2 forms a thiyl cation (RSH^+) that is further converted into a radical molecule, as portrayed in Scheme 6. Some thiol/alkene combinations resulted in high yields and definitively, this work presents an interesting perspective on RS^\bullet generation from dispersed nanoparticles. In a similar work, Bi_2O_3 photocatalyst powders were used; again, BrCCl_3 was used to generate trichloromethyl radicals for thiyl radical production.⁵² Nonetheless, in both cases, mechanistic studies of these chemical transformations involving nanoparticles are still missing and represent an exciting field of research.

2.2.2 Photochemical thiol-ene click reactions in materials science

2.2.2.1 Synthesis of molecular precursors and molecular building blocks: organoalkoxysilanes. Since the introduction of the click chemistry concept, the copper-catalyzed azide-alkyne cycloaddition (CuAAC) reaction was one of its most popular



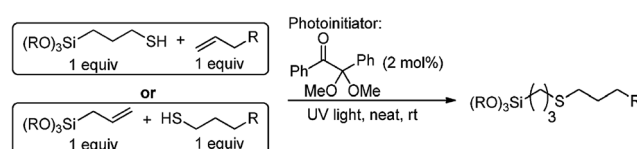
Scheme 6 Proposed mechanistic pathway for TiO_2 mediated PRTEA reaction. Reproduced under Creative Commons Attribution 3.0 Unported License from Bhat *et al.*, *Chem. Commun.*, 2015, **51**, 4383–4385.

reactions.^{53,54} This reaction easily binds azide and alkyne groups covalently, resulting in a 1,4-disubstituted-1,2,3-triazole linker that can be adapted to polymers and various surfaces.⁵⁴ The SiO_2 sol-gel derived materials community has largely benefited from using this chemical reaction, as this procedure enables the synthesis of water-sensitive molecular alkoxysilanes precursors with modest resources.^{55–58} However, the CuAAC reaction poses a great risk because azide derived products are potentially explosive precursors. In this context, PRTEA emerged as a very useful and extensively used click reaction for polymer modification, finding other applications, from the synthesis of radio-pharmaceutical derivatives for biological imaging and targeting, to glycoconjugation modifications.^{59–62}

In a seminal work, Garrell *et al.* introduced a series of alkoxysilanes synthesized under UV light, using neat mixtures of 3-mercaptopropyltrialkoxysilane and an allyl/terminal alkene, or a thiol and allyltrialkoxysilane, in the presence of 2 mol% of DMPA (Irgacure® 651) as a photoinitiator, shown in Scheme 7.⁶³

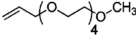
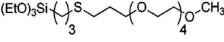
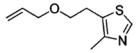
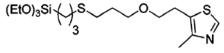
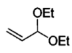
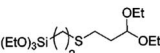
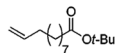
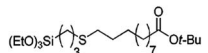
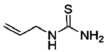
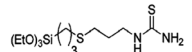
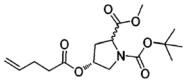
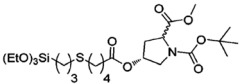
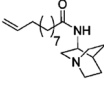
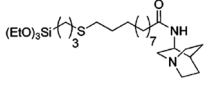
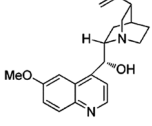
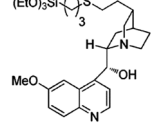
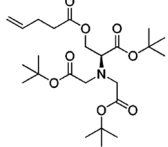
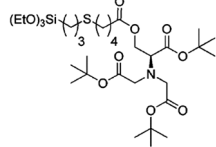
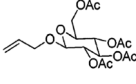
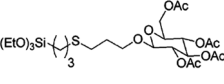
As a characteristic feature of thiol-ene addition reactions, $^1\text{H-NMR}$ vinyl carbons signals from unreacted alkenes ($\delta \sim 6.5$ – 5.8 ppm) are non-existent or extremely weak, pointing to almost complete conversions of the $\text{C}=\text{C}$ bond into thioether. Typical conversions lie in the 94% to >99% range, while the purity of the obtained silanes is well above 90%, as seen in Table 1.

Moreover, these authors provide a cost analysis for the synthesis of specific precursors, finding that it is possible to



Scheme 7 Trialkoxysilanes precursors synthesis using PRTEA. Reproduced with permission from Tucker-Schwartz *et al.*, *J. Am. Chem. Soc.*, 2011, **133**, 11026–11029. Copyright 2011 American Chemical Society.

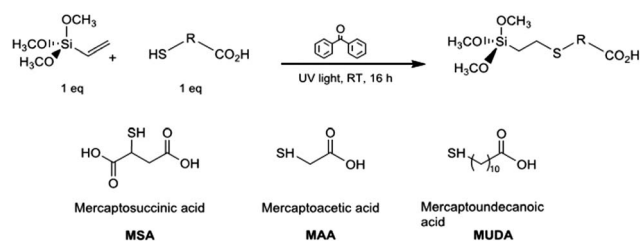
Table 1 Triethoxysilanes library from PRTEA between mercaptopropylsilanes and various alkenes. Reproduced with permission from Tucker-Schwartz *et al.*, *J. Am. Chem. Soc.*, 2011, **133**, 11026–11029. Copyright 2011 American Chemical Society

Alkene	Triethoxysilane		Conv. (%)	Purity (%)
		1	>99	96
		2	>99	95
		3	>99	96
		4	98	96
		5	>99	95
		6	96	94
		7	98	96
		8	98	96
		9	94	90
		10	>99	97

lower the retail price of silane derivatives from usual chemical suppliers to 1/13. Although they do not provide information related to scaling-up energetic costs (*i.e.* UV), the simplicity for getting tailored alkoxy silanes stands out as a remarkable feature of the PRTEA reaction.

Based on this work, we introduced a general approach for anchoring carboxylic groups on SiO₂ materials, an elusive chemical group in silica modification (see Scheme 8).^{64,65} The ¹H-NMR of crude PRTEA reactions of mercaptosuccinic acid, mercaptoundecanoic acid and mercaptoacetic acid with vinyltrimethoxysilane show the appearance of a signal at high fields ($\delta \sim 0.9$ ppm), due to methylene protons bonded to Si ($-\text{Si}-\text{CH}_2-\text{CH}_2-\text{S}-\text{CH}_2$) after the formation of a thioether bond.

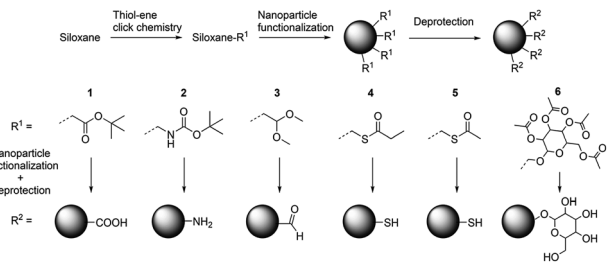
Along this line, Bloemen *et al.* described the use of the PRTEA click chemistry to synthesize various different siloxanes with protected functional groups. The SiO– bonds anchor to the surface of iron oxide NPs and are deprotected later on. In this way, they solve the issues of colloidal stability and wrong ligand orientations (*i.e.* Fe₃O₄ has affinity for –COOH groups) as represented in Scheme 9.⁶⁶ Fine chemical tuning of the SiO₂/



Scheme 8 PRTEA carboxylic derivatized silanes from thioacids and vinyltrimethoxysilane. Reproduced with permission from Bordoni *et al.*, *J. Colloid Interface Sci.*, 2015, **450**, 316–324. Copyright 2015 Elsevier B. V.

magnetic oxides interface is extremely important when aiming for imaging biomedical applications.¹⁵

In a recent example, Carron *et al.* used this strategy for developing bimodal contrast agents for MRI and optical imaging. They reacted a macrocyclic allyl derivative of DO3A-*t*-butyl ester with the modified surface of ultra-small Fe₃O₄ nanoparticles with 3-mercaptopropyltrialkoxysilane. The DO3A



Scheme 9 Siloxanes with protected groups. Deprotection leads to carboxylic acids (1), amines (2), aldehydes (3), thiols, (4, 5) and sugars (6). Reproduced with permission from Bloemen *et al.*, *Chem-PlusChem*, 2015, **80**, 50–53. Copyright 2015 Wiley-VCH Verlag GmbH & Co. KGaA.

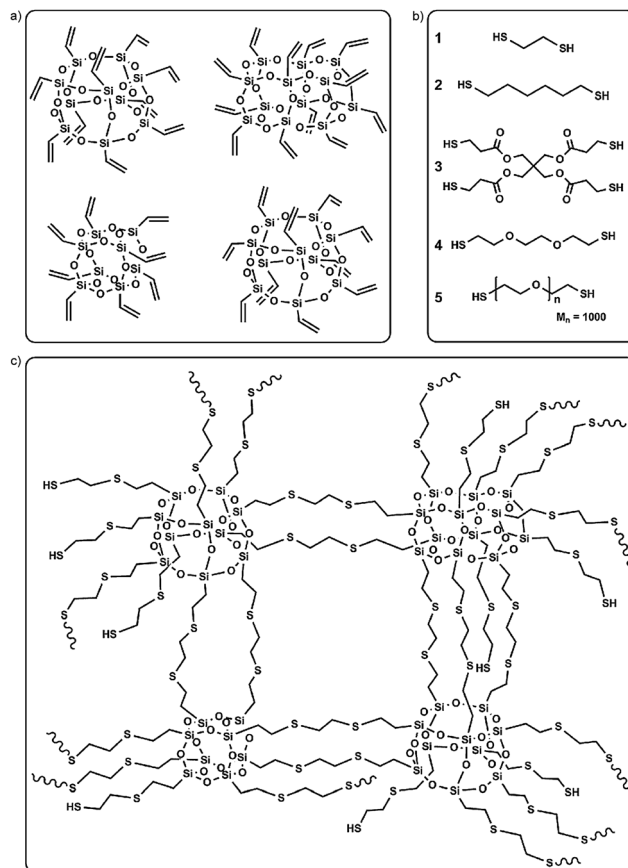
organic moiety anchored on the Fe₃O₄ surface entrapped Eu(III) ions; characterization of the relaxometric and optical properties of the bimodal system was conducted. This work demonstrates the usefulness of PTREA in the synthesis of complex organic siloxane-coating precursors with simple building blocks.⁶⁷

The generation of biocompatible surfaces for medical applications requires the anchoring molecules with high affinity for bio-membranes. Phosphorylcholine (PC) is a major component of eukaryotic cell membranes; PC derivatives show high affinity for living organs and present an excellent perspective as antifouling surface modifiers for medical applications.⁶⁸ Starting from allylphosphorylcholine, Liu *et al.* synthesized trimethoxy-, triethoxy-, dimethylethoxy- and methyldiethoxy-silane precursors and concluded that the thio-ether linkage provides less steric effects, therefore higher loading rates on SiO₂ surfaces, when compared with the CuAAC reaction, involving bulkier triazole moieties.

2.2.2.2 Polyhedral oligomeric silsesquioxanes precursors (POSS). Among the family of sol-gel SiO₂ precursors, polyhedral oligomeric silsesquioxanes (POSS) have Si_nO_{3n/2}R_n stoichiometry with cage-like nanostructures that show chemical diversity and increasing use as building blocks for the generation of porous materials and nanoparticles.⁶⁹ Alves and Nischang prepared porous organic-inorganic monolithic materials employing vinyl-POSS and multi-functional thiols *via* PRTEA, as shown in Scheme 10.⁷⁰

Interestingly, FT-IR Raman experiments suggest that some thiol moieties remain unreacted and susceptible for further modification; on the other hand, no vinyl alkene signals were detected. We hypothesize that as the alkene/thiol ratio used in their experiments is 1 : 1.5, the excess thiol may become entrapped within the monolithic structure. Nonetheless, the vinyl-POSS linker thiol library was explored, shown in Scheme 10, and resulted in monoliths with variable degrees of hydrophobicity/hydrophilicity and mechanical properties (gels to rigid materials) (Fig. 1).⁷⁰

Liu *et al.* explored the PRTEA reaction between monovinyl substituted POSS and a series of thiols bearing hydroxyl, carboxyl, ester and trialkoxysilane groups to produce the corresponding functionalized POSS monomers; yields ranged in the 85% to 99% using DMPA as a PI.⁷¹



Scheme 10 Vinyl-POSS (RSiO_{3/2})_n with (a) $n = 8, 10, 12$; (b) thiol compounds; and (c) hybrid SiO₂ materials prepared from the PRTEA reaction between vinyl-POSS (a) and thiol compounds (b). Reproduced under Creative Commons Attribution License from Alves *et al.*, *Chem. Eur. J.*, 2013, **19**, 17310–17313.

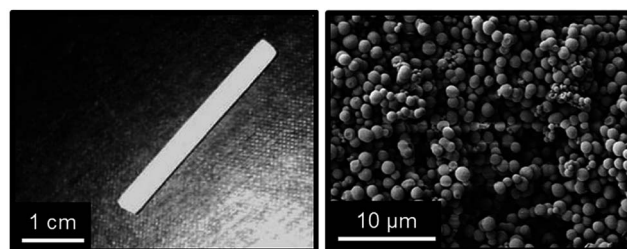
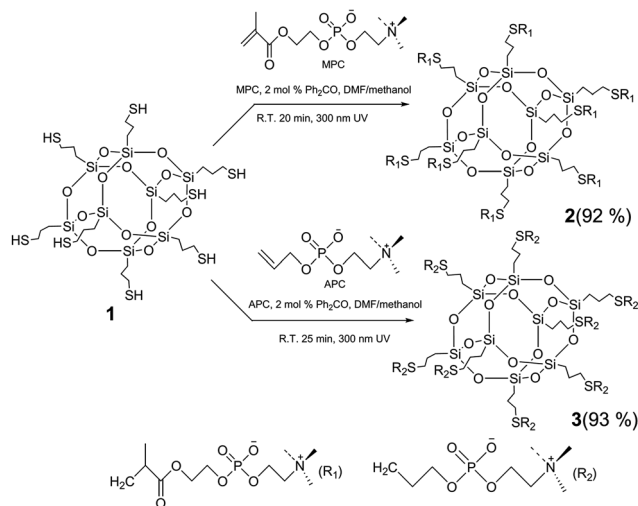


Fig. 1 SiO₂ monolith prepared from vinyl-POSS and dithiol linkers prepared in quartz glass tubes using PRTEA: optical photograph (left) and scanning electron microscopy micrograph (right). Reproduced under Creative Commons Attribution License from Alves *et al.*, *Chem. Eur. J.*, 2013, **19**, 17310–17313.

As we have seen before, phosphorylcholine is a highly attractive chemical group for tissue engineering applications. With the perspective of the design of new biomedical POSS hybrids, phosphorylcholine-substituted silsesquioxanes were synthesized between octakis(3-mercaptopropyl)octasilsesquioxane (POSS-SH) with 2-methacryloyloxyethyl-phosphorylcholine or allyl-phosphorylcholine as depicted in Scheme 11 (yields >93%).⁷²

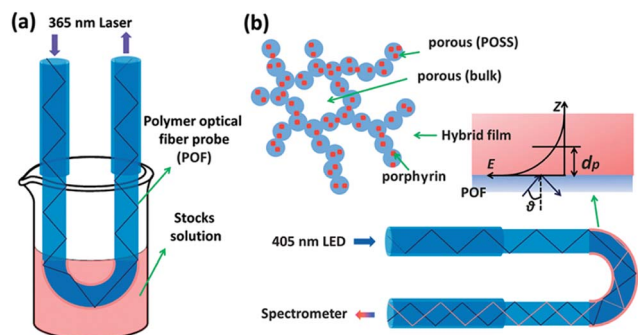


Scheme 11 Syntheses of phosphorylcholine-substituted silsesquioxanes via PRTEA. Reproduced with permission from Liu *et al.*, *Tetrahedron Lett.* 2015, **56**, 1562–1565. Copyright 2015 Elsevier B.V.

In a nice example of *in situ* PRTEA synthesis of a sol-gel film, Zhang and co-workers, irradiated with evanescent UV light the surface of a U-bent poly(methyl methacrylate) optical fiber submerged in a solution containing vinyl-functionalized polyhedral oligomeric silsesquioxanes (POSS-V8), alkane dithiols, a fluorescent allylporphyrin and DMPA (Scheme 12).⁷³ This resulted in a facile strategy to fabricate fluorescent porous oxide thin films for vapor phase sensing of TNT explosives.

Zhao and Xu, reported the synthesis of various POSS-SiO₂ porous aerogels with potential applications in oil/water separation processes and sound absorption materials; vinyl-trimethoxy-, vinyltriethoxy-, mercaptopropyltrimethoxy- and mercaptopropyltriethoxysilanes reacted in the presence of DMPA as PI.⁷⁴

Han and co-workers synthesized regioisomeric Janus-type polyhedral POSS using two consecutive PRTEA.⁷⁵ Starting from octavinyl-POSS and β -mercaptoethanol, they obtained a mixture



Scheme 12 (a) Fabrication process of TNT sensitive optical device and (b) schematic of U-bent POF probe. A 365 nm laser is used for PRTEA synthesis of a POSS sol-gel film. The 405 nm diode laser is selected for excitation of the porphyrin sensor molecule. Reproduced with permission from Ma *et al.*, *ACS Appl. Mater. Interfaces*, 2015, **7**, 241–249. Copyright 2015 American Chemical Society.

of [2 : 6] octakis-adducts, which were separated using flash chromatography.

Fang *et al.* introduced an interesting approach for the synthesis of inorganic-organic hybrid POSS fibers by integrating UV initiated thiol-ene polymerization and centrifugal fiber spinning.⁷⁶ The authors remarked on the enhanced thermal and mechanical fiber properties due to the POSS cage structure.

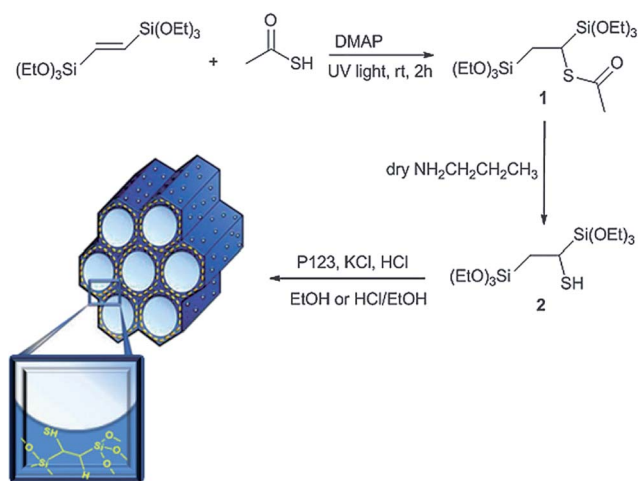
2.2.2.3 Non-siliceous transition metal-oxo clusters. Transition metal-oxo clusters are well-characterized species in the sol-gel chemistry field, with sizes ranging from 0.5 to 2.5 nm.¹⁰ These chemical units are excellent nano-sized building blocks with defined organic functional groups on the outer shell of the inorganic cluster. Engineering of the shell allows the formation of covalent bonds with organic polymer frameworks, while the core metal-oxo cluster may have magnetic, electronic or catalytic properties.^{10,77}

In 2007, Gross and co-workers, reported the first application of PRTEA on a thiol-functionalized zirconium oxocluster with the purpose of a polymer-hybrid material. They showed that the organic-inorganic oxoclusters were well dispersed within the polymeric network, with no significant macroscopic agglomeration. Increasing the Zr oxoclusters content also increased T_g values, storage modulus in the rubbery region, and thermal stability of the polymeric hybrid material. XPS analysis and SIMS depth profile confirmed the homogeneous distribution of these clusters within the polymeric matrix.⁷⁸ An ensuing paper reported two isostructural mercapto-functionalized zirconium- and hafnium-oxoclusters $[M_{12}(\mu_3-O)_8(\mu_3-OH)_8(MP)_{24} \cdot n(MPA)]$, MPA = HS-(CH₂)₂-C(O)OH; MP = HS-(CH₂)₂-C(O)O-; M = Zr, Hf; $n = 4$ for Zr, $n = 5$ for Hf], which were included in a poly-methacrylic matrix using PRTEA.⁷⁹

2.2.2.4 SiO₂ mesoporous materials. Mesoporous materials constitute an attractive framework for the immobilization of functional groups, due to the high surface area/mass ratio. The advantageous simple synthesis of silane-based precursors opens a simple modification pathway and the tailoring of porous materials.^{63,64} Typically, the functionalization of mesoporous oxide based materials can be achieved according to the following approaches: post-synthetic grafting or co-condensation of oxide precursors and functional groups.⁸⁰

Esquivel *et al.* synthesized a thiol functionalized bis-silane PMO precursor between 1,2-(*E*)-bis(triethoxysilyl)ethane and thioacetic acid (see Scheme 13).⁸¹ After aminolysis, the self-assembly process of the formed SH-precursor with Pluronic® P123, under acidic conditions, yielded a 2D-hexagonal (*P6mm*) mesostructured PMO with good structural ordering. In particular, co-condensation of this bis-silane within the SiO₂ framework resulted in free thiols and disulphide bridges, as evidenced by ¹³C CP/MAS NMR and FT-Raman spectra. In a continuing work, this group oxidized the SH groups to SO₃H for acid catalysis and found that not all thiol groups are accessible to oxidation, as usually observed when using the co-condensation approach of organoalkoxysilanes for mesoporous matrices chemical modification.⁸²

Taking advantage of the immobilized ethylene bridges in the previous PMO framework, Ouwehand *et al.* obtained a series of

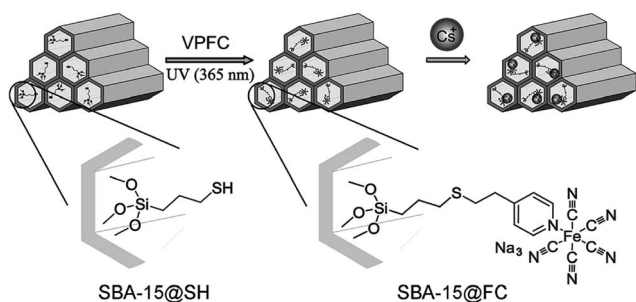


Scheme 13 Synthesis of 1-thiol-1,2-bis(triethoxysilyl)ethane (2) and its corresponding thiol periodic mesoporous silica material (SH-PMO). Reproduced from ref. 81 with permission from the Royal Society of Chemistry.

acid–base catalysts.⁸³ The PRTEA reaction allowed them to graft, in a simple manner, cysteamine and cysteine. In the latter case, antagonistic acid and base groups were incorporated into a single postgrafting step, without using protecting groups or several synthetic steps.

The high surface area/mass ratio of mesoporous materials is a valuable feature for adsorbents design. In this context, SBA-15 SiO₂ powders are versatile frameworks for easy chemical modification. Qian *et al.* synthesized a Cs⁺ adsorbent using the PRTEA between thiol-modified SBA-15 and a pentacyano(4-vinylpyridine)ferrate complex, as shown in Scheme 14. The anchored Fe complex endured several recycling adsorption/desorption cycles, indicating the strength of the thioether bond.⁸⁴

Bordoni *et al.* modified SBA-15 with COOH groups from PRTEA between mercaptosuccinic acid, mercaptoundecanoic acid, mercaptoacetic acid and vinyltrimethoxysilane keeping the original mesoporosity (see Fig. 2). All post-grafted groups



VPFC: Pentacyano(4-vinylpyridine)ferrate complex

Scheme 14 Synthesis of the Prussian blue derivate-modified mesoporous material (SBA-15@FC) via PRTEA for cesium adsorption. Reproduced with permission from Qian *et al.*, *Chemistry, an Asian journal*, 2015, 10, 1738–1744. Copyright 2015 Wiley-VCH Verlag GmbH & Co. KGaA.

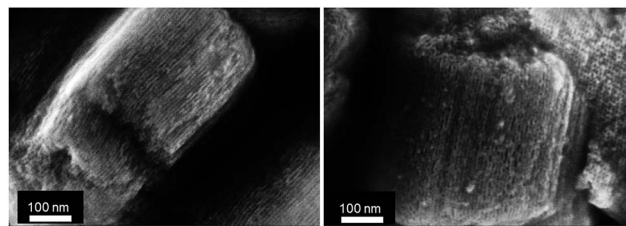
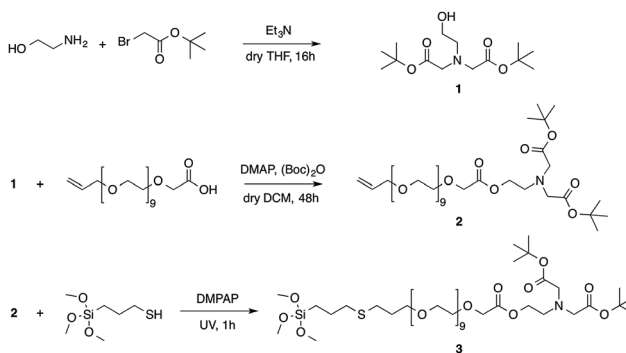


Fig. 2 Scanning electronic micrographs of SBA-15 modified with mercaptosuccinic acid through PRTEA. Reproduced with permission from Bordoni *et al.*, *J. Colloid Interface Sci.*, 2015, 450, 316–324. Copyright 2015 Elsevier B. V.

were available for Cu²⁺ adsorption and chemically accessible as evidenced from COO[−] and COOH FTIR signals.⁶⁴

2.2.2.5 Nanoparticles. Chemical tailoring of nanoparticle surfaces has become a common practice for numerous practical reasons: (a) preventing particle coagulation, (b) driving and sensing of specific molecular recognition events, (c) promoting chemical stability (avoiding or minimizing etching processes) and (d) modulating physical properties of core particles (*e.g.* plasmon bands in metallic NP). The synthesis of organoalkoxysilanes as SiO₂ molecular precursors represents a unique opportunity for nanoparticle synthesis or precise SiO₂ shell engineering for core–shell particles.^{85,86}

Silica shells modulate magnetic interactions in superparamagnetic Fe₃O₄ NP and provide an ideal anchorage for covalent bonding of specific ligands.^{87,88} Bloemen and coworkers modified oleic-Fe₃O₄ nanoparticles with an hetero-bifunctional methoxysilane, for covalent Fe₃O₄ surface attachment, and with an iminodiacetic end group for Ni²⁺ chelation. This is a well-known strategy for recovering genetically engineered His tagged proteins from cell lysates.⁸⁹ Moreover, adding a polyethyleneglycol chain (PEG) provided excellent colloidal stability of superparamagnetic particles in aqueous solutions (Scheme 15).



Scheme 15 Synthetic steps for imidoacetic (IDA) PEGylated silane molecule. The functionalized ethanolamine (1) is covalently bonded to PEG via an ester bond forming an allyl-PEG-imidoacetic-*t*Bu molecule (2). PRTEA between 2 and mercaptopropylsilane leads to an IDA siloxane precursor. Posterior hydrolysis of the ester groups in 3 results in a free IDA moiety. Reproduced from ref. 89 with permission from the Royal Society of Chemistry.

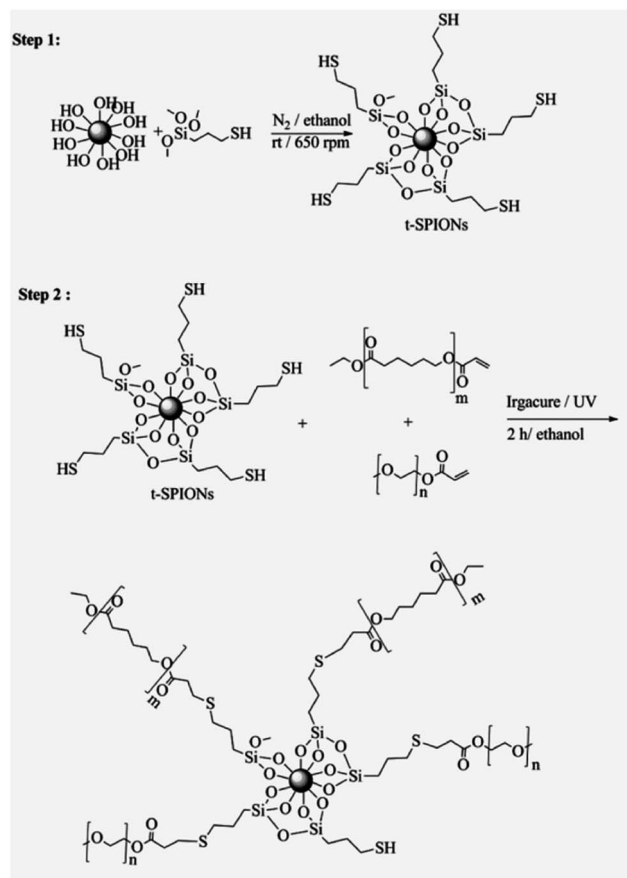
When designing magnetically recoverable transition metal adsorbents, Fe_3O_4 surfaces represent a chemical challenge, as they are TMO themselves, sharing the same chemistry as SiO_2 surfaces. For example, diphosphonic acid is a highly desirable ligand for heavy metals, lanthanides, and actinides separation (see Scheme 16); unfortunately, the diphosphonate moiety also possesses a high affinity for iron oxide surfaces. This limits the probability of having free phosphonate groups oriented to the solution. Warner and co-workers solved this issue by joining an allyl diphosphonic molecule to mercaptopropionic modified Fe_3O_4 NPs under UV light, using BP as photoinitiator.⁹¹ Also, in a recent publication, they used the same family of ligands for uranium extraction from seawater.⁹¹

Khoei *et al.* synthesized superparamagnetic iron oxide nanoparticles (SPIONs) for cancer drug delivery with balanced hydrophilic/hydrophobic surface energy.⁹² This group anchored (3-mercaptopropyl)-trimethoxysilane on the SPION surface, obtaining a thiol-decorated NP, which further reacted, *via* PRTEA, with an acrylated poly(caprolactone) (PCL, hydrophobic) and methoxy poly(ethylene glycol) (PEG, hydrophilic) as represented in Scheme 17. This resulted in two types of polymers on the surface of the SPIONs, which could be modeled by employing coarse grain methods. Tuning the surface ratio of the PEG and PCL improved drug loading, cellular internalization and colloidal stability.

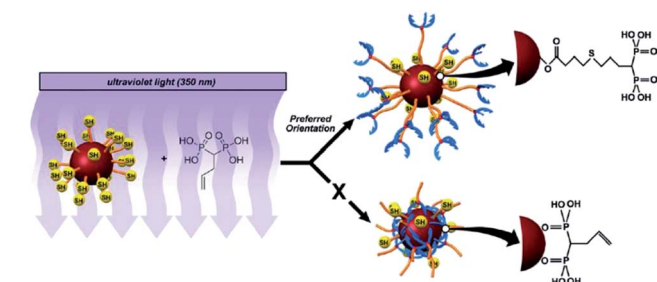
Liang *et al.* combined the superparamagnetism of Fe_3O_4 nanoparticles and the electrocatalytic activity of ferrocene for developing a recyclable, magneto-controlled bioelectrocatalytic system for glucose oxidation.⁹³ The switching of the biocatalytic activity and recyclable usage of the ferrocene functionalized NP by means of the external magnet could provide a simple, green and convenient strategy for bioelectrosensing. Thiol-terminated Fe_3O_4 nanoparticles were synthesized and further reacted with vinylferrocene under 365 nm UV.

Amici *et al.* synthesized poly(ethylene glycol) coated Fe_3O_4 nanoparticles using vinyltrimethoxysilane for surface oxide modification and further PRTEA with poly(ethylene glycol) dithiol with no photoinitiator.⁹⁴ The obtained particles were well distributed and not aggregated, with an average size of about 20–50 nm, as shown by TEM and DLS analyses.

Georgiadou *et al.* synthesized CoFe_2O_4 NPs stabilized with oleylamine (OAm), which further reacted with free thiols of



Scheme 17 Synthesis of PEG and PCL polymers on mercaptopropylsilane modified magnetite NPs. Reproduced from ref. 92 with permission from the Royal Society of Chemistry.



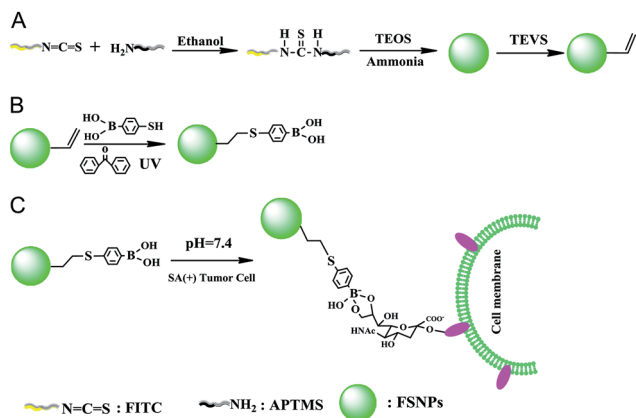
Scheme 16 PRTEA based strategy for avoiding undesirable headgroup anchoring orientation of phosphonate ligands on Fe_3O_4 nanoparticles. Reproduced with permission from Rutledge *et al.*, *Langmuir*, 2010, 26, 12285–12292. Copyright 2010 American Chemical Society.

bovine serum albumin modified with fluorescein (FITC-BSA).⁹⁵ The hydrophobic OAm- CoFe_2O_4 NP had to be phase transferred with CTAB for the PRTEA reaction with UV/DMPA.

Cheng *et al.* described the synthesis of fluorescent SiO_2 nanoparticles with boronic moieties for labelling overexpressed sialic acid in tumorous cell surface glycan structures.⁹⁶ Mercaptoboronic acid was covalently bound through a PRTEA to vinyl-modified SiO_2 NP as exemplified in Scheme 18. The labelling specificity on living cells was investigated by flow cytometry and confocal laser scanning microscopy.

Ruizendaal *et al.* introduced a PRTEA procedure for obtaining ultra-small silicon nanoparticles (SiNP, radius < 5 nm) with tailored chemical groups.⁹⁷ Thiol-ene chemistry performed on these surfaces allowed having functional SiNPs terminated with thioacetic acid, mercaptoethanol, ethylene glycol, and carboxylic acid. In addition to their nontoxicity, Si NPs have optical properties comparable to conventional quantum dots.

Silver-free antibacterial surfaces are promising environmentally friendly materials for controlling adhesion and the growth of pathogenic microorganisms. Gehring *et al.* obtained highly porous thiol-functionalized nanoparticles that were modified with vinyl-derivatized Rose Bengal using PRTEA and NO anchoring through forming a *S*-nitrosothiol bond.⁹⁸



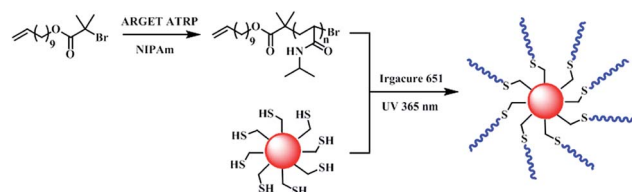
Scheme 18 Synthesis of phenylboronic acid-tagged fluorescent silica nanoparticles, PBA-FSNPs, and their application for specific labeling of sialic acid on living cancer cells. (A) Preparation of vinyl-FSNPs by a reverse microemulsion technique, (B) surface modification of FSNPs with thiol-PBA tags using PRTEA, and (C) specific labeling of cellular sialic acid using PBA-FSNPs. Reproduced with permission from Cheng *et al.*, *Talanta* 2013, **115**, 823–829. Copyright 2013 Elsevier B.V.

Sunlight triggered both the production of singlet O_2 and the release of NO, having a synergistic effect for biocidal activity.

Although there is a wide library of alkene-derived and thiol simple molecules, highly designed polymeric materials constitute interesting modular building blocks for nanoparticle and plain surface modification. Polymer chemical diversity provides another way for tuning the physicochemical properties of various interfaces, an extremely important feature when designing stimuli-responsive surfaces, sensors and supramolecular delivery systems.

There are considerable efforts in the polymer science area focused on PRTEA as a synthetic technique for obtaining new thioether-based monomers that are susceptible to (co)polymerisation by a range of established methods, as well as a method for the modification of proper side- or end-group (co) polymers.^{23,59} For instance, reversible addition-fragmentation chain transfer (RAFT) polymerization processes involve the use of dithioesters, trithioesters and thiolcarbonyl as chain transfer agents. These chemical groups are readily converted into thiol moieties under mild reductive aqueous conditions, opening the possibility to be combined with PRTEA.⁹⁹ Moreover, atom transfer radical polymerization (ATRP) is another preferred method as thiol functional groups can be introduced, modifying the halide end groups of the ATRP polymer.¹⁰⁰

Mai *et al.* combined PRTEA and “activators regenerated by electron transfer atom transfer radical polymerization” (ARGET ATRP) for developing a thermo-responsive core-shell nanosystem based on poly(*N*-isopropylacrylamide) (PNIPAm) and SiO_2 nanoparticles. ARGET ATRP was used as a reaction key for building the clickable precursor of PNIPAm (alkene counterpart), thiol functionalized silica nanoparticles were also synthesized as the complementary part and PRTEA was used for clicking the two blocks, as depicted in Scheme 19. The PNIPAm SiO_2 nanoparticles showed thermo-responsive behaviour and may be useful for developing future stimuli-responsive delivery systems.¹⁰¹

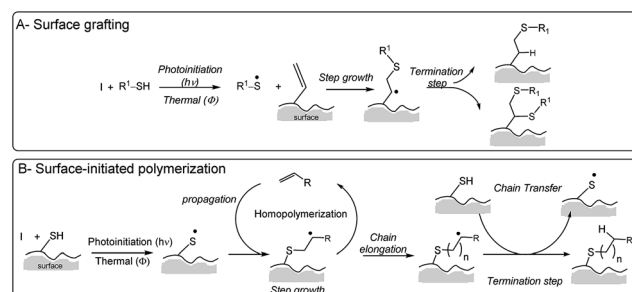


Scheme 19 Synthetic approach to the preparation of PNIPAm-*g*- SiO_2 nanocomposites by the combination of click chemistry and ARGET ATRP. Reproduced with permission from Mai *et al.*, *Journal of Materials Science*, 2014, **49**, 1519–1526. Copyright 2014 Springer US.

Recently, Wu *et al.* obtained hyperbranched polymer-functionalized powders combining SiO_2 nanoparticles treated with 3-mercaptopropyl trimethoxysilane to introduce mercapto groups, and successive trimethylolpropane triacrylate (TMPTA) and trimethylolpropane tris 3-mercaptopropionate (Trithol) using the PRTEA reaction.¹⁰² Although the reaction scheme is interesting and resembled a dendronized surface, no precautions were taken in order to avoid SiO_2 nanoparticle agglomeration.

2.2.2.6 Monolith synthesis and chemical modification. The isolation and chromatographic separation of molecules in complex mixtures needs simple chemical modification procedures of the stationary phases.¹⁰³ Although there is a vast body of work on radical thiol-ene reactions, PRTEA offers a unique opportunity of low temperature and localized chemical modification.¹⁰³ In this context, Marechal and co-workers coined the “ene-thiol” photografting approach, highlighting the case where free thiols in solution add to surface anchored vinyl groups. The RS^\bullet attacks the vinyl group tethered to the silica surface, forming the thioether bond. As only one vinyl group is able to react with two thiol molecules, this reaction is better considered as a grafting reaction and not as polymerization. On the other hand, this group refers to “thiol-ene” when surface bound thiols react with vinyl compounds in solution, as presented in Scheme 20.¹⁰⁴ In this case, the free vinyl monomers may polymerize in solution first and then react with the thiol functions on the monolith surface. Polymerization on the stationary phase surface leads to clogged chromatographic columns, diminishing analyte permeability and separation efficiency.

As an example of a rational material design approach, Laaniste *et al.* obtained a reversed-phase SiO_2 monolithic column

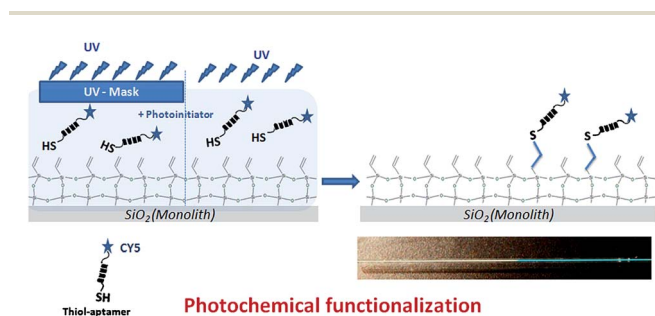


Scheme 20 Schematic of “ene-thiol” (A) and “thiol-ene” reaction (B) proposed by Laaniste *et al.*¹⁰⁴ Adapted from ref. 104.

with high permeability when they reacted 1-octadecanethiol with the vinyl pre-functionalized silica monolith surface.¹⁰⁴ This same group developed a multimodal biphasic monolithic column using successive photografting reactions with a UV-mask to localize different surface chemistries. Using different thiol monomers (octadecanethiol, cysteine and sodium mercaptoethanesulfonate), they prepared capillary columns with multiple chromatographic modes (reversed-phase, hydrophilic interaction and strong cation exchange) that were able to pre-concentrate and separate β -blocker molecules.¹⁰⁵ Moreover, they designed an aptamer-photoclicked silica monolith for in-line enrichment and purification of ochratoxin A, a suspected carcinogenic mycotoxin.¹⁰⁶ In particular, a vinyl spacer was used for PRTEA anchoring of 5'-SH-modified oligonucleotide aptamers under irradiation at 365 nm for five minutes. Photografting allowed the confinement of the binding reaction to the desired silica monolithic segment, while the rest of the monolith was used for capillary electrophoresis. Both instances constitute good examples of anchoring and localizing specific chemical groups for molecular separation and detection (Fig. 3).

Cheng *et al.* carried out the PRTEA between 3-mercaptopropyltriethoxysilane (MPTES) and diethyl vinylphosphonate (DEVP) for nucleoside separations as shown in Scheme 21.¹⁰⁷ The modified SiO₂ colloidal particles were packed and employed in both reversed-phase liquid chromatography (RPLC) mode and hydrophilic interaction liquid chromatography (HILIC) mode.

We have mentioned that is unusual to report the degree of monolith or surface modification after thiol-ene click-based reactions. However, Göbel *et al.* carried on a meticulous study on thiol-, vinyl- and allyl-modified mesoporous SiO₂ monoliths.¹⁰⁸ The alkene double bond content present in SiO₂ monoliths were determined from iodine titrations and compared to ²⁹Si solid-state NMR spectroscopy, elemental analysis and thermal gravimetric analysis. In particular, they found post-grafting efficiencies in the range of 25 to 50%, due to crowding of chemical groups on pore surfaces or non-accessible functional groups within the mesoporous structure.¹⁰⁸ Demesmay and coworkers extended this analysis comparing reactions like bromination, radical initiated thiol-ene addition, PRTEA



Scheme 21 Chromatographic phosphate ester-bonded silica stationary phase synthesis. Reproduced with permission from Cheng *et al.*, *J. Chromatogr. A*, 2013, **1302**, 81–87. Copyright 2015 Elsevier B.V.

and radical initiated bisulfite reaction, observing a similar behaviour.¹⁰⁹ Overall, for post-grafting mesopores chemical modification, there is a limit on the PRTEA ligation efficiency that depends on the following: (i) the steric constraints imposed by nanosized pore pockets and (ii) the unequal chemistry, according to which surface group is anchored (thiol-ene or ene-thiol).^{104,110}

2.2.2.7 Planar Si/SiO₂ modified surfaces. The photopatterning of Si/SiO₂ surfaces is crucial for the development of biosensors and high throughput biomolecular screening devices. As part of the “-omics revolution”, where genomics, proteomics and metabolomics have reshaped the experimental design and analysis, microarray technologies are able to produce highly reproducible, easily fabricated and robust bioassay platforms for point-of-care diagnosis and drug discovery.¹¹¹ Simple conventional photolithography procedures, that assure reliable and controlled molecule/probe anchoring procedures, highly benefit from direct attachment without using cross-linkers (one-pot fashion) and short irradiation times.

Escorihuela *et al.* developed a rapid strategy for the covalent immobilization of DNA onto silicon-based materials using the PRTEA.¹¹² They demonstrated that thiol- and alkene-modified oligonucleotide probes were covalently attached in microarray format with immobilization densities of around 6 pmol cm⁻², in 20 minutes, without the addition of photoinitiators.

Li *et al.* reported the generation of chemically hydrophilic micropatterns prepared on trichlorovinylsilane superhydrophobic glass substrates using the PRTEA without PI.¹¹³

Han *et al.* also reported the use of fluorinated 1H,1H,2H-perfluoro-1-octene bonded to mercaptopropylsilane modified SiO₂. X-ray photoelectron spectroscopy studies indicated the successful conversion of surface functionality.¹¹⁴

Köwitsch *et al.* demonstrated that glycosaminoglycans (GAG) on SiO₂ glass slides resulted in a biocompatible surface for growing human fibroblasts.¹¹⁵ The authors reacted thiolated-GAG with 7-octenyldimethylchlorosilane modified SiO₂ slides and proposed the applications of GAG modified surfaces for studies on cell adhesion and migration.

The photochemical reaction can be also employed for nanoparticle immobilization on planar surfaces. Aerosol bifunctional mesoporous nanoparticles, containing thiol and

Fig. 3 Localization of the PRTEA reaction using UV and a photomask. Photograph of a capillary column after photografting of a thiol-modified and blue labeled oligonucleotide (poly(T)10). The UV-masked monolith segment remains white after washing, while the UV exposed segment is blue. Reproduced with permission from Marechal *et al.*, *J. Chromatogr. A*, 2015, **1406**, 109–117. Copyright 2015 Elsevier B.V.

sulfonic acid groups, were anchored to allyltrimethoxysilane glass slides under direct UV illumination at 365 nm for 1 hour.¹¹⁶ The immobilized particles were solidly attached while the remaining SH groups immobilized within the pores, held Ag NPs with biocide activity.

Poly(ionic liquid)s (PILs) were anchored onto alkene modified SiO₂ surfaces using DMPA as PI for 30 minutes.¹¹⁷ Clickable PILs were synthesized from styrenic imidazolium ionic liquid monomer through ATRP containing thiol terminal groups. PIL end groups are proposed for “smart” surfaces, anti-bacterial and anti-biofouling applications.

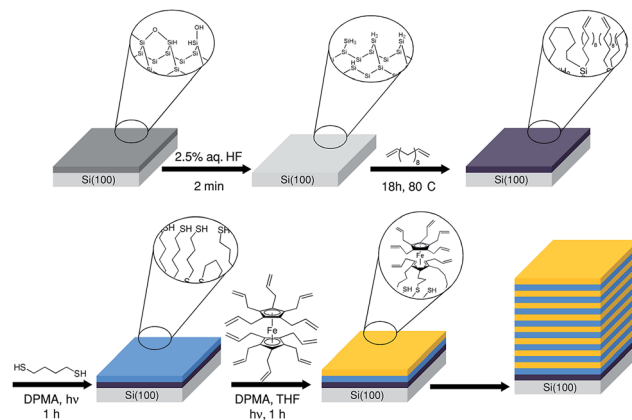
Tan *et al.* took on a rigorous study on the efficiency of the PRTEA compared to the corresponding thiol-yne reaction, analysing immobilized ATRP-generated polyglycidyl methacrylate (PGMA) polymer brushes on glass slides and Si wafers.¹¹⁸ PGMA surfaces were modified with various thiols (cysteamine, *N*-acetyl-L-cysteine, *etc.*) via direct photo-irradiation through a photomask and reactive microcontact printing. The density of the polymer brushes was found to confine functionalisation to its outermost surface, presumably due to restricted molecular diffusion.

Siloxane units and silica nanoparticles offer the opportunity to texturize glass slides with superhydrophobic properties.¹¹⁹ Uniform coatings obtained by spray-deposition of UV-curable hybrid inorganic-organic thiol-ene resins consisting of pentaerythritol tetra(3-mercaptopropionate) (PETMP), triallyl isocyanurate (TTT), 2,4,6,8-tetramethyl-2,4,6,8-tetravinylcyclotetrasiloxane (TMTVSi), and hydrophobic fumed silica nanoparticles. In this particular case, the spray-deposition process and nanoparticle agglomeration/dispersion provided a surface with hierarchical structure with both micro- and nanoscale roughness. The surface photomodification was done under 6 minutes using a UV lamp. This same process was later adapted for the hydrophobization of a metallic mesh for oil/water separation.¹²⁰

Chemtob *et al.* combined two photoinduced orthogonal reactions, PRTEA and alkoxy-silyl sol-gel condensation using a photoacid generator, that converged in the fast formation of thioether-siloxane nanocomposite films.¹²¹ The formation of a rigid oxo-polymer siloxane network with high crosslink density coexists with the thiol-ene coupling, which imparts flexibility, elasticity and resistance to the cracking of the final material.

Silicon surfaces are interesting platforms for molecular-based electronics. Schulz *et al.* immobilized on highly doped p-type silicon (100), in a layer-by-layer approach, electroactive allyl-modified ferrocene (decaallyl-ferrocene, DAFc) with neat 1,4-butanedithiol utilizing thiol-ene click reaction conditions (see Scheme 22).¹²² Photoactivation was done using DMPA and a blue LED; the build-up of the redox system followed a linear growth.

Bhairamadgi *et al.* compared thru XPS analysis the degree of Si surface functionalization for a wide range of thiol structures.¹²³ Interestingly, they found that in a thiol-alkyne reaction, at least one thiol molecule reacted per alkyne group; on the other hand, for the PRTEA reaction, these values were lower: on average, 0.5 thiol molecules reacted per alkene moiety on an

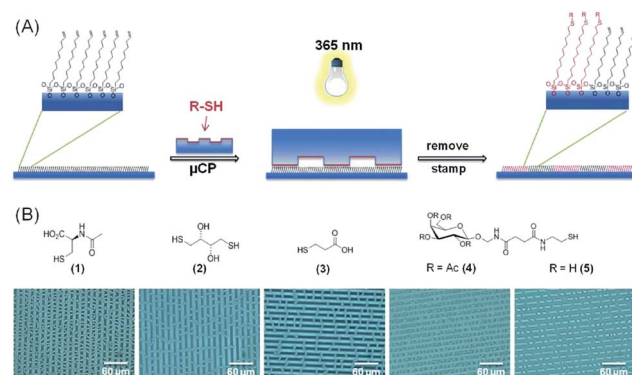


Scheme 22 Surface modification of Si (100) and subsequent covalent layer-by-layer deposition using PRTEA. Reproduced with permission from Schulz *et al.*, *Small*, 2012, 8, 569–577. Copyright 2012 Wiley-VCH Verlag GmbH & Co. KGaA.

alkene-terminated monolayer. Only when anchoring a bulky functional group, such as the *N*-Fmoc-protected form of L-cysteine, did both photochemical thiol-ene and thiol-yne reactions modify the silicon substrate to an equal degree.

In conclusion, molecular crowding and steric repulsions on surfaces jeopardize highly efficient homogeneous chemical reactions; these molecular events reshape the click terminology, limiting the original concept.^{19,20}

2.2.2.8 Microcontact printed surfaces. We have mentioned that the production of chemically patterned surfaces has a tremendous impact in all biological applications that require high throughput screening microarrays, such as proteomics or DNA based sensors. However, the surface immobilization of biomolecules needs gentle chemical and physical techniques for surface anchoring to avoid denaturation of their native

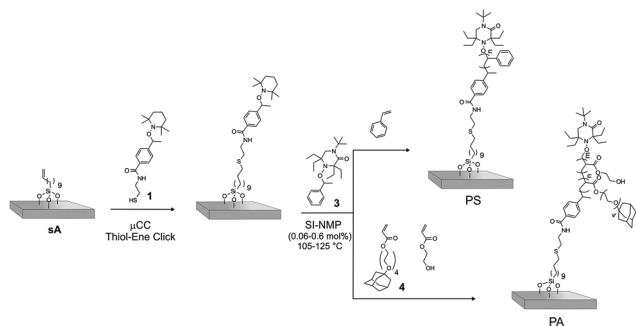


Scheme 23 (A) PRTEA μ CP: an oxidized PDMS stamp inked with a thiol is placed on an alkene-terminated substrate (glass slides or Si (100) buffered with native oxide) and irradiated with 365 nm UV light. Covalent bonding of the thiol occurs exclusively in the stamp's area of contact. (B) Light microscopy images of water condensation experiments on surfaces patterned by printing *N*-acetyl-L-cysteine (1), D,L-dithiothreitol (2), 3-mercaptopropionic acid (3), tetraacetylgalactoside-thiol conjugate (4), and galactoside-thiol conjugate (5). Reproduced with permission from Wendeln *et al.*, *Langmuir*, 2010, 26, 15966–15971. Copyright 2010 American Chemical Society.

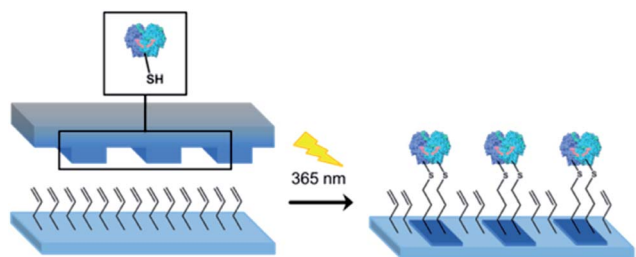
structures or the compromise of their enzymatic activity.¹²⁴ Microcontact printing (μ CP) is an exceptional tool for obtaining biocompatible substrates, in opposition to photolithography that requires harsh conditions or complicated steps.¹²⁵ The μ CP approach relies on a polydimethylsiloxane (PDMS) stamp that is “inked” with molecules of interest and placed on a reactive substrate; in this way, only the stamp’s area of contact modifies the substrate surface as shown in Scheme 23. This is convenient for “biological ink” components like carbohydrates, proteins and nucleic acids, which are usually available only in small quantities.¹²⁶

Several groups combined the PRTEA with μ CP techniques on flat surfaces, obtaining low cost and highly reproducible biocompatible surfaces with a high throughput production.^{126–133} As a matter of fact, it has been shown that photochemical μ CP yields dense monolayers of functional molecules under times as short as 30 s.¹²⁶

Roling *et al.* demonstrated the immobilization of a microcontacted thiol-alkoxyamine nitroxide-mediated polymerization initiator on an undecenyl modified glass by PRTEA and combined surface-initiated nitroxide-mediated polymerization of polystyrene (SI-NMP), represented in Scheme 24.¹³⁴ This resulted in patterned polystyrene (PS) and polyacrylate (PA) brushes for site-selective protein immobilization.



Scheme 24 Synthesis of patterned PS and PA polymer brushes using PRTEA combined with μ CP for immobilizing surface-initiated nitroxide-mediator for polymerization.¹³⁴ Reproduced with permission from Roling *et al.*, *Macromolecules*, 2014, 47, 2411–2419. Copyright 2014 American Chemical Society.



Scheme 25 Enzyme immobilization on glass slides using PRTEA μ CP. Fluorescence microscopy of GOx-FITC printed in 5 μ m dots, spaced by 3 μ m. Scale bar: 50 μ m. Reproduced with permission from Buhl *et al.*, *Bioconjugate Chem.*, 2015, 26, 1017–1020. Copyright 2015 American Chemical Society.

Recently, Ravoo and co-workers patterned glucose oxidase and lactase enzymes on octenyltrichlorosilane or undecenyltrichlorosilane modified glass slides.¹³⁵ Given that both enzymes have free thiol groups (cysteines) in their native structure, they achieved direct enzyme anchoring to the alkene-modified SiO₂ surface without additional steps like enzyme modification or the use of coupling reagents (Scheme 25).

3. Conclusions and future perspectives

We can conclude that the PRTEA is a “revamped” reaction for easy surface modification of materials and synthesis of organoalkoxysilane precursors. The simple experimental setup, compared to other highly popular click-based reactions (*e.g.* CuAAC), the possibility to carry the reaction at low temperatures and synthetic orthogonality configure a versatile tool for the synthesis and modification of molecular building blocks. Simple photoinitiation of the thiol-alkene addition emerges as a highly attractive feature for spatial and temporal synthesis of chemical precursors and surface modification. As the pore surface functionalization of SiO₂ and TMO mesoporous materials with organoalkoxysilanes imparts chemical properties that can be directed to gating and controlled delivery (“smart triggered” platforms), adsorbents catalysis and separation, PRTEA is a valuable tool for easy grafting of tailored molecules. Moreover, in terms of flexibility, this approach can be extended to other materials and rapid surface prototyping (*i.e.* μ CP), providing control over the interfacial chemistry.

Despite the highly attractive features of the PRTEA as a “mix-and-use” reaction, some issues should be widened. For instance, fundamental studies have shown that the chemical diversity of the thiol group forces a careful analysis of reaction conditions in the “preclick” preparative steps.^{20,27} This same kind of analysis should be applied in the materials science area; the chemistry of the anchoring sites on the surfaces of porous and non-porous oxide materials can have a definite impact on either the kinetic or thermodynamic parameters of the reaction. Highly confined surfaces, as mesoporous oxide frameworks, deserve special attention as they can alter surface acid–base equilibria or impose steric constraints.^{136,137} Unfortunately, detailed studies and analysis of the PRTEA yields and stoichiometry on surfaces are scarce and rarely performed. These observations should be paired with theoretical calculations; quantum chemical studies of the PRTEA in solution have already described experimental results very well.²⁷ We anticipate the combination of experimental and theoretical approaches in order to get a complete picture of the whole process.

PRTEA certainly accounts as a click metal-free alternative to CuAAC when it comes to biomedical and biomaterial applications. Triazole units, present in the CuAAC approach, are known to complex Cu, raising serious concerns for biological uses. As we have seen, several research groups have embraced the PRTEA approach as a safer alternative for labelling and conjugation of biomolecules (proteins, enzymes, carbohydrates, DNA). Nonetheless, this option suffers from an uncomfortable

shortcoming because even after brief expositions, high-energy UV photons may compromise the molecular integrity of the biomolecules due to light induced side-reactions (*i.e.* variations in enzymatic parameters or denaturation). In this context, the use of long wavelength (low energy photons) PI represents an excellent perspective for “soft” radical initiation. Anyhow, the fate of PRTEA photoinitiators after materials synthesis and surface modification is still pending.

Light is an exceptional external trigger for initiating the catalytic process of the PRTEA; localized illumination, photo-masks and very recently, the development of nanoparticle-based photoinitiators offer extraordinary opportunities for achieving extremely localized chemistry. It is highly likely that these features, in conjunction with surface immobilization techniques, will help the growing research on organic chemical reactions in microfluidic setups or flow reactors. Moreover, easy custom-made polymers with –ene or thiol end groups, obtained through reliable and well-established organic synthesis approaches (*i.e.* ATRP and RAFT), will expand the universe of macromolecular building blocks for producing high-end modified TMO surfaces through PRTEA, a relatively unexplored area.

In summary, PRTEA adds to the existing library for simple surface functionalization with molecules, nanomaterials synthesis and substrate chemical patterning. Evidently, this approach intertwines the design of molecular building blocks with well-defined chemical and physical properties, building up a multidisciplinary effort with a far-reaching impact in various technological and scientific applications.

Acknowledgements

M. V. L. acknowledges a postdoctoral fellowship from CONICET. A. V. B. and A. W. are permanent research fellows of CONICET. We thank C.F.K and N.K. for 12 years of continuous moral inspiration. This work was funded in part by ANPCyT (PICT 2012-2087, PICT 2013-1303) and CONICET (PIP 12201030000121).

References

- 1 C. Sanchez, P. Belleville, M. Popall and L. Nicole, *Chem. Soc. Rev.*, 2011, **40**, 696–753.
- 2 M. F. Montemor, *Surf. Coat. Technol.*, 2014, **258**, 17–37.
- 3 M. M. Stevens and J. H. George, *Science*, 2005, **310**, 1135–1138.
- 4 L. Lili, Z. Xin, R. Shumin, Y. Ying, D. Xiaoping, G. Jinsen, X. Chunming and H. Jing, *RSC Adv.*, 2014, **4**, 13093–13107.
- 5 A. Walcarius and L. Mercier, *J. Mater. Chem.*, 2010, **20**, 4478–4511.
- 6 S. Nishimoto and B. Bhushan, *RSC Adv.*, 2013, **3**, 671–690.
- 7 S. Alberti, G. J. A. A. Soler-Illia and O. Azzaroni, *Chem. Commun.*, 2015, **51**, 6050–6075.
- 8 Q. Zhang and F. Wei, *Advanced Hierarchical Nanostructured Materials*, Wiley, 2014.
- 9 G. Kickelbick, *Hybrid Materials: Synthesis, Characterization, and Applications*, Wiley, 2007.
- 10 B. Charleux, C. Coperet and E. Lacote, *Chemistry of Organohybrids: Synthesis and Characterization of Functional Nano-Objects*, Wiley, 2015.
- 11 M. Pagliaro, *Silica-based Materials for Advanced Chemical Applications*, RSC Pub., 2009.
- 12 P. Gómez-Romero and C. Sanchez, *Functional hybrid materials*, John Wiley & Sons, 2006.
- 13 H. Wei, Y. Wang, J. Guo, N. Z. Shen, D. Jiang, X. Zhang, X. Yan, J. Zhu, Q. Wang, L. Shao, H. Lin, S. Wei and Z. Guo, *J. Mater. Chem. A*, 2015, **3**, 469–480.
- 14 R. A. Sheldon and S. Van Pelt, *Chem. Soc. Rev.*, 2013, **42**, 6223–6235.
- 15 Z. Li, J. C. Barnes, A. Bosoy, J. F. Stoddart and J. I. Zink, *Chem. Soc. Rev.*, 2012, **41**, 2590–2605.
- 16 D. Arcos and M. Vallet-Regí, *Acta Biomater.*, 2010, **6**, 2874–2888.
- 17 B. Lebeau and P. Innocenzi, *Chem. Soc. Rev.*, 2011, **40**, 886–906.
- 18 R. Ciriminna, A. Fidalgo, V. Pandarus, F. Béland, L. M. Ilharco and M. Pagliaro, *Chem. Rev.*, 2013, **113**, 6592–6620.
- 19 H. C. Kolb, M. G. Finn and K. B. Sharpless, *Angew. Chem., Int. Ed.*, 2001, **40**, 2004–2021.
- 20 P. Espeel and F. E. Du Prez, *Macromolecules*, 2015, **48**, 2–14.
- 21 J. Lahann, *Click Chemistry for Biotechnology and Materials Science*, Wiley, 2009.
- 22 C. Barner-Kowollik, F. E. Du Prez, P. Espeel, C. J. Hawker, T. Junkers, H. Schlaad and W. Van Camp, *Angew. Chem., Int. Ed.*, 2011, **50**, 60–62.
- 23 C. E. Hoyle, A. B. Lowe and C. N. Bowman, *Chem. Soc. Rev.*, 2010, **39**, 1355–1387.
- 24 C. R. Morgan, F. Magnotta and A. D. Ketley, *J. Polym. Sci., Polym. Chem. Ed.*, 1977, **15**, 627–645.
- 25 J. C. Love, L. A. Estroff, J. K. Kriebel, R. G. Nuzzo and G. M. Whitesides, *Chem. Rev.*, 2005, **105**, 1103–1169.
- 26 C. E. Hoyle, T. Y. Lee and T. Roper, *J. Polym. Sci., Part A: Polym. Chem.*, 2004, **42**, 5301–5338.
- 27 B. H. Northrop and R. N. Coffey, *J. Am. Chem. Soc.*, 2012, **134**, 13804–13817.
- 28 L. T. T. Nguyen, M. T. Gokmen and F. E. Du Prez, *Polym. Chem.*, 2013, **4**, 5527–5536.
- 29 D. P. Nair, M. Podgórski, S. Chatani, T. Gong, W. Xi, C. R. Fenoli and C. N. Bowman, *Chem. Mater.*, 2014, **26**, 724–744.
- 30 C. Decker and T. Nguyen Thi Viet, *J. Appl. Polym. Sci.*, 2000, **77**, 1902–1912.
- 31 N. Herzer, S. Hoepfener and U. S. Schubert, *Chem. Commun.*, 2010, **46**, 5634–5652.
- 32 A. Waldbaur, H. Rapp, K. Lange and B. E. Rapp, *Anal. Methods*, 2011, **3**, 2681–2716.
- 33 F. Dénès, M. Pichowicz, G. Povie and P. Renaud, *Chem. Rev.*, 2014, **114**, 2587–2693.
- 34 J. P. Fouassier and J. Lalevée, *Photoinitiators for Polymer Synthesis: Scope, Reactivity, and Efficiency*, Wiley, 2013.
- 35 W. A. Green, *Industrial Photoinitiators: A Technical Guide*, CRC Press, 2010.
- 36 N. S. Allen, J. Segurola, M. Edge, E. Santamari, A. McMahon and S. Wilson, *Surf. Coat. Int.*, 1999, **82**, 67–76.

- 37 T. Gong, B. J. Adzima and C. N. Bowman, *Chem. Commun.*, 2013, **49**, 7950–7952.
- 38 M. A. Tehfe, F. Dumur, B. Graff, F. Morlet-Savary, J. P. Fouassier, D. Gigmes and J. Lalevée, *Macromolecules*, 2013, **46**, 3761–3770.
- 39 P. Xiao, F. Dumur, B. Graff, D. Gigmes, J. P. Fouassier and J. Lalevée, *Macromolecules*, 2014, **47**, 601–608.
- 40 J. Zhang, M. Frigoli, F. Dumur, P. Xiao, L. Ronchi, B. Graff, F. Morlet-Savary, J. P. Fouassier, D. Gigmes and J. Lalevée, *Macromolecules*, 2014, **47**, 2811–2819.
- 41 J. Zhang, N. Zivic, F. Dumur, P. Xiao, B. Graff, D. Gigmes, J. P. Fouassier and J. Lalevée, *J. Polym. Sci., Part A: Polym. Chem.*, 2015, **53**, 445–451.
- 42 M. A. Tehfe, F. Dumur, P. Xiao, M. Delgove, B. Graff, J. P. Fouassier, D. Gigmes and J. Lalevée, *Polym. Chem.*, 2014, **5**, 382–390.
- 43 J. Shao, Y. Huang and Q. Fan, *Polym. Chem.*, 2014, **5**, 4195–4210.
- 44 R. A. Angnes, Z. Li, C. R. D. Correia and G. B. Hammond, *Org. Biomol. Chem.*, 2015, **13**, 9152–9167.
- 45 C. K. Prier, D. A. Rankic and D. W. C. MacMillan, *Chem. Rev.*, 2013, **113**, 5322–5363.
- 46 M. H. Keylor, J. E. Park, C. J. Wallentin and C. R. J. Stephenson, *Tetrahedron*, 2014, **70**, 4264–4269.
- 47 J. Xu and C. Boyer, *Macromolecules*, 2015, **48**, 520–529.
- 48 W. Ma, D. Chen, L. Liu, Y. Ma, L. Wang, C. Zhao and W. Yang, *J. Polym. Sci., Part A: Polym. Chem.*, 2016, **54**, 740–749.
- 49 X. Lang, X. Chen and J. Zhao, *Chem. Soc. Rev.*, 2014, **43**, 473–486.
- 50 J. Chen, J. Cen, X. Xu and X. Li, *Catal. Sci. Technol.*, 2016, **6**, 349–362.
- 51 V. T. Bhat, P. A. Duspara, S. Seo, N. S. B. Abu Bakar and M. F. Greaney, *Chem. Commun.*, 2015, **51**, 4383–4385.
- 52 O. O. Fadeyi, J. J. Mousseau, Y. Feng, C. Allais, P. Nuhant, M. Z. Chen, B. Pierce and R. Robinson, *Org. Lett.*, 2015, **17**, 5756–5759.
- 53 L. Liang and D. Astruc, *Coord. Chem. Rev.*, 2011, **255**, 2933–2945.
- 54 J. F. Lutz, *Angew. Chem., Int. Ed.*, 2008, **47**, 2182–2184.
- 55 X. Cattoën, A. Nouredine, J. Croissant, N. Moitra, K. Bürglová, J. Hodačová, O. De Los Cobos, M. Lejeune, F. Rossignol, D. Toulemon, S. Bégin-Colin, B. P. Pichon, L. Raehm, J. O. Durand and M. Wong Chi Man, *J. Sol-Gel Sci. Technol.*, 2014, **70**, 245–253.
- 56 N. Moitra, J. J. Moreau, X. Cattoën and M. W. C. Man, *Chem. Commun.*, 2010, **46**, 8416–8418.
- 57 K. n. Bürglová, N. Moitra, J. Hodačová, X. Cattoën and M. Wong Chi Man, *J. Org. Chem.*, 2011, **76**, 7326–7333.
- 58 A. Nouredine, L. Lichon, M. Maynadier, M. Garcia, M. Gary-Bobo, J. I. Zink, X. Cattoën and M. Wong Chi Man, *Nanoscale*, 2015, **7**, 11444–11452.
- 59 A. B. Lowe, *Polym. Chem.*, 2014, **5**, 4820–4870.
- 60 T. R. Hayes, P. A. Lyon, E. Silva-Lopez, B. Twamley and P. D. Benny, *Inorg. Chem.*, 2013, **52**, 3259–3267.
- 61 A. Dondoni and A. Marra, *Chem. Soc. Rev.*, 2012, **41**, 573–586.
- 62 M. Fiore, A. Marra and A. Dondoni, *J. Org. Chem.*, 2009, **74**, 4422–4425.
- 63 A. K. Tucker-Schwartz, R. A. Farrell and R. L. Garrell, *J. Am. Chem. Soc.*, 2011, **133**, 11026–11029.
- 64 A. V. Bordoni, M. V. Lombardo, A. E. Regazzoni, G. J. A. A. Soler-Illia and A. Wolosiuk, *J. Colloid Interface Sci.*, 2015, **450**, 316–324.
- 65 L. Han, O. Terasaki and S. Che, *J. Mater. Chem.*, 2011, **21**, 11033–11039.
- 66 M. Bloemen, B. Sutens, W. Brulot, A. Gils, N. Geukens and T. Verbiest, *ChemPlusChem*, 2015, **80**, 50–53.
- 67 S. Carron, M. Bloemen, L. Vander Elst, S. Laurent, T. Verbiest and T. N. Parac-Vogt, *Chem.–Eur. J.*, 2016, **22**, 4521–4527.
- 68 L. Liu, S. J. Park, J. H. Park and M. E. Lee, *RSC Adv.*, 2015, **5**, 14273–14276.
- 69 K. Tanaka and Y. Chujo, *J. Mater. Chem.*, 2012, **22**, 1733–1746.
- 70 F. Alves and I. Nischang, *Chem.–Eur. J.*, 2013, **19**, 17310–17313.
- 71 L. Li, L. Xue, S. Feng and H. Liu, *Inorg. Chim. Acta*, 2013, **407**, 269–273.
- 72 L. Liu, S. J. Lee, M. E. Lee, P. Kang and M. G. Choi, *Tetrahedron Lett.*, 2015, **56**, 1562–1565.
- 73 J. Ma, L. Lv, G. Zou and Q. Zhang, *ACS Appl. Mater. Interfaces*, 2015, **7**, 241–249.
- 74 Z. Wang, D. Wang, Z. Qian, J. Guo, H. Dong, N. Zhao and J. Xu, *ACS Appl. Mater. Interfaces*, 2015, **7**, 2016–2024.
- 75 S. Y. Han, X. M. Wang, Y. Shao, Q. Y. Guo, Y. Li and W. B. Zhang, *Chem.–Eur. J.*, 2016, **22**, 6397–6403.
- 76 Y. Fang, H. Ha, K. Shanmuganathan and C. J. Ellison, *ACS Appl. Mater. Interfaces*, 2016, **8**, 11050–11059.
- 77 S. Gross, *J. Mater. Chem.*, 2011, **21**, 15853–15861.
- 78 M. Sangermano, S. Gross, A. Priola, G. Rizza and C. Sada, *Macromol. Chem. Phys.*, 2007, **208**, 2560–2568.
- 79 F. Faccini, H. Fric, U. Schubert, E. Wendel, O. Tsetsgee, K. Müller, H. Bertagnolli, A. Venzo and S. Gross, *J. Mater. Chem.*, 2007, **17**, 3297–3307.
- 80 A. Mehdi, C. Reye and R. Corriu, *Chem. Soc. Rev.*, 2011, **40**, 563–574.
- 81 D. Esquivel, O. Van Den Berg, F. J. Romero-Salguero, F. Du Prez and P. Van Der Voort, *Chem. Commun.*, 2013, **49**, 2344–2346.
- 82 M. I. López, D. Esquivel, C. Jiménez-Sanchidrián, F. J. Romero-Salguero and P. Van Der Voort, *J. Catal.*, 2015, **326**, 139–148.
- 83 J. Ouweland, J. Lauwaert, D. Esquivel, K. Hendrickx, V. Van Speybroeck, J. W. Thybaut and P. Van Der Voort, *Eur. J. Inorg. Chem.*, 2016, **2016**, 2144–2151.
- 84 J. Qian, J. Ma, W. He and D. Hua, *Chem.–Asian J.*, 2015, **10**, 1738–1744.
- 85 M. Ohmori and E. Matijević, *J. Colloid Interface Sci.*, 1992, **150**, 594–598.
- 86 P. Mulvaney, L. M. Liz-Marzán, M. Giersig and T. Ung, *J. Mater. Chem.*, 2000, **10**, 1259–1270.
- 87 A. P. Philipse, M. P. B. Van Bruggen and C. Pathmamanoharan, *Langmuir*, 1994, **10**, 92–99.

- 88 S. Wei, Q. Wang, J. Zhu, L. Sun, H. Lin and Z. Guo, *Nanoscale*, 2011, **3**, 4474–4502.
- 89 M. Bloemen, L. Vanpraet, M. Ceulemans, T. N. Parac-Vogt, K. Clays, N. Geukens, A. Gils and T. Verbiest, *RSC Adv.*, 2015, **5**, 66549–66553.
- 90 R. D. Rutledge, C. L. Warner, J. W. Pittman, R. S. Addleman, M. Engelhard, W. Chouyyok and M. G. Warner, *Langmuir*, 2010, **26**, 12285–12292.
- 91 W. Chouyyok, J. W. Pittman, M. G. Warner, K. M. Nell, D. C. Clubb, G. A. Gill and R. S. Addleman, *Dalton Trans.*, 2016, **45**, 11312–11325.
- 92 S. Khoei, Y. Bagheri and A. Hashemi, *Nanoscale*, 2015, **7**, 4134–4148.
- 93 C. Liang, L. Jing, X. Shi, Y. Zhang and Y. Xian, *Electrochim. Acta*, 2012, **69**, 167–173.
- 94 J. Amici, P. Allia, P. Tiberto and M. Sangermano, *Macromol. Chem. Phys.*, 2011, **212**, 1629–1635.
- 95 V. Georgiadou, C. Kokotidou, B. Le Droumaguet, B. Carbonnier, T. Choli-Papadopoulou and C. Dendrinou-Samara, *Dalton Trans.*, 2014, **43**, 6377–6388.
- 96 L. Cheng, X. Zhang, Z. Zhang, H. Chen, S. Zhang and J. Kong, *Talanta*, 2013, **115**, 823–829.
- 97 L. Ruizendaal, S. P. Pujari, V. Gevaerts, J. M. J. Paulusse and H. Zuilhof, *Chem.–Asian J.*, 2011, **6**, 2776–2786.
- 98 J. Gehring, B. Trepka, N. Klinkenberg, H. Bronner, D. Schleheck and S. Polarz, *J. Am. Chem. Soc.*, 2016, **138**, 3076–3084.
- 99 R. Fu and G.-D. Fu, *Polym. Chem.*, 2011, **2**, 465–475.
- 100 C. Boyer, A. H. Soeriyadi, P. J. Roth, M. R. Whittaker and T. P. Davis, *Chem. Commun.*, 2011, **47**, 1318–1320.
- 101 T. B. Mai, T. N. Tran, M. Rafiqul Islam, J. M. Park and K. T. Lim, *J. Mater. Sci.*, 2014, **49**, 1519–1526.
- 102 J. Wu, G. Ma, L. Ling and B. Wang, *Polym. Bull.*, 2016, **73**, 859–873.
- 103 A. Marechal, R. El-Debs, V. Dugas and C. Demesmay, *J. Sep. Sci.*, 2013, **36**, 2049–2062.
- 104 A. Laaniste, A. Marechal, R. El-Debs, J. Randon, V. Dugas and C. Demesmay, *J. Chromatogr. A*, 2014, **1355**, 296–300.
- 105 A. Marechal, A. Laaniste, R. El-Debs, V. Dugas and C. Demesmay, *J. Chromatogr. A*, 2014, **1365**, 140–147.
- 106 A. Marechal, F. Jarroson, J. Randon, V. Dugas and C. Demesmay, *J. Chromatogr. A*, 2015, **1406**, 109–117.
- 107 X. D. Cheng, X. T. Peng, Q. W. Yu, B. F. Yuan and Y. Q. Feng, *J. Chromatogr. A*, 2013, **1302**, 81–87.
- 108 R. Göbel, P. Hesemann, A. Friedrich, R. Rothe, H. Schlaad and A. Taubert, *Chem.–Eur. J.*, 2014, **20**, 17579–17589.
- 109 R. El-Debs, F. Cadoux, L. Bois, A. Bonhommé, J. Randon, V. Dugas and C. Demesmay, *Langmuir*, 2015, **31**, 11649–11658.
- 110 J. Escorihuela, A. T. M. Marcelis and H. Zuilhof, *Adv. Mater. Interfaces*, 2015, **2**, 1500135.
- 111 V. Romanov, S. N. Davidoff, A. R. Miles, D. W. Grainger, B. K. Gale and B. D. Brooks, *Analyst*, 2014, **139**, 1303–1326.
- 112 J. Escorihuela, M. J. Bañuls, S. Grijalvo, R. Eritja, R. Puchades and A. Maquieira, *Bioconjugate Chem.*, 2014, **25**, 618–627.
- 113 J. Li, L. Li, X. Du, W. Feng, A. Welle, O. Trapp, M. Grunze, M. Hirtz and P. A. Levkin, *Nano Lett.*, 2015, **15**, 675–681.
- 114 X. Han, C. Wu and S. Sun, *Appl. Surf. Sci.*, 2012, **258**, 5153–5156.
- 115 A. Köwitsch, M. Jurado Abreu, A. Chhalotre, M. Hielscher, S. Fischer, K. Mäder and T. Groth, *Carbohydr. Polym.*, 2014, **114**, 344–351.
- 116 J. Gehring, D. Schleheck, B. Trepka and S. Polarz, *ACS Appl. Mater. Interfaces*, 2015, **7**, 1021–1029.
- 117 H. He, S. Averick, E. Roth, D. Luebke, H. Nulwala and K. Matyjaszewski, *Polymer*, 2014, **55**, 3330–3338.
- 118 K. Y. Tan, M. Ramstedt, B. Colak, W. T. S. Huck and J. E. Gautrot, *Polym. Chem.*, 2016, **7**, 979–990.
- 119 B. J. Sparks, E. F. T. Hoff, L. Xiong, J. T. Goetz and D. L. Patton, *ACS Appl. Mater. Interfaces*, 2013, **5**, 1811–1817.
- 120 Q. Chen, A. De Leon and R. C. Advincula, *ACS Appl. Mater. Interfaces*, 2015, **7**, 18566–18573.
- 121 A. Chemtob, H. De Paz-Simon, M. Sibeaud, B. El Fouhali, C. Croutxé-Barghorn, L. Jacomine, C. Gauthier and V. Le Houérou, *eXPRESS Polym. Lett.*, 2016, **10**, 439–449.
- 122 C. Schulz, S. Nowak, R. Fröhlich and B. J. Ravoo, *Small*, 2012, **8**, 569–577.
- 123 N. S. Bhairamadgi, S. Gangarapu, M. A. Caipa Campos, J. M. J. Paulusse, C. J. M. Van Rijn and H. Zuilhof, *Langmuir*, 2013, **29**, 4535–4542.
- 124 G. T. Hermanson, *Bioconjugate Techniques*, Elsevier Science, 2013.
- 125 T. Kaufmann and B. J. Ravoo, *Polym. Chem.*, 2010, **1**, 371–387.
- 126 C. Wendeln, S. Rinnen, C. Schulz, H. F. Arlinghaus and B. J. Ravoo, *Langmuir*, 2010, **26**, 15966–15971.
- 127 M. A. C. Campos, J. M. J. Paulusse and H. Zuilhof, *Chem. Commun.*, 2010, **46**, 5512–5514.
- 128 J. Mehlich and B. J. Ravoo, *Org. Biomol. Chem.*, 2011, **9**, 4108–4115.
- 129 O. Roling, C. Wendeln, U. Kauscher, P. Seelheim, H. J. Galla and B. J. Ravoo, *Langmuir*, 2013, **29**, 10174–10182.
- 130 D. Wasserberg, T. Steentjes, M. H. W. Stopel, J. Huskens, C. Blum, V. Subramaniam and P. Jonkheijm, *J. Mater. Chem.*, 2012, **22**, 16606–16610.
- 131 C. Wendeln and B. J. Ravoo, *Langmuir*, 2012, **28**, 5527–5538.
- 132 C. Wendeln, S. Rinnen, C. Schulz, T. Kaufmann, H. F. Arlinghaus and B. J. Ravoo, *Chem.–Eur. J.*, 2012, **18**, 5880–5888.
- 133 D. Weinrich, M. Köhn, P. Jonkheijm, U. Westerlind, L. Dehmelt, H. Engelkamp, P. C. M. Christianen, J. Kuhlmann, J. C. Maan, D. Nüsse, H. Schröder, R. Wacker, E. Voges, R. Breinbauer, H. Kunz, C. M. Niemeyer and H. Waldmann, *ChemBioChem*, 2010, **11**, 235–247.
- 134 O. Roling, A. Mardyukov, J. A. Krings, A. Studer and B. J. Ravoo, *Macromolecules*, 2014, **47**, 2411–2419.
- 135 M. Buhl, B. Vonhören and B. J. Ravoo, *Bioconjugate Chem.*, 2015, **26**, 1017–1020.
- 136 A. A. Gurinov, D. Mauder, D. Akcakayiran, G. H. Findenegg and I. G. Shenderovich, *ChemPhysChem*, 2012, **13**, 2282–2285.
- 137 A. Calvo, P. C. Angelomé, V. M. Sánchez, D. A. Scherlis, F. J. Williams and G. J. A. A. Soler-Illia, *Chem. Mater.*, 2008, **20**, 4661–4668.